ORIGINAL PAPER

Synthesis, characterization, and in vitro antibacterial activity of some new pyridinone and pyrazole derivatives with some in silico ADME and molecular modeling study

Khadija E. Saadon[1] · Nadia M. H. Taha[1] · N. A. Mahmoud[1] · Gameel A. M. Elhagali[2] · Ahmed Ragab[2]

Abstract

A new series of pyridine-2-one and pyrazole derivatives were designed and synthesized based on cyanoacrylamide derivatives containing 2,4-dichlro aniline and 6-methyl 2-amino pyridine as an aryl group. Condensation of cyanoacrylamide derivatives **3a–d** with different active methylene (malononitrile, ethyl cyanoacetate cyanoacetamide, and ethyl acetoacetate) in the presence of piperidine as basic catalyst afforded the corresponding pyridinone derivatives **4a–c**, **5**, **9**, and **13**. Furthermore, the reaction of cyanoacrylamide derivatives **3a–d** with bi-nucleophile as hydrazine hydrate and thiosemicarbazide afforded the corresponding pyrazole derivatives **14a,b** and **16**. The newly designed derivatives were confirmed and established based on the elemental analysis and spectra data (IR, ^{1}H NMR, ^{13}C NMR, and mass). The in vitro antibacterial activity was evaluated against four bacterial strains with weak to good antibacterial activity. Moreover, the results indicated that the most active derivatives **3a**, **4a**, **4b**, **9**, and **16** might lead to antibacterial agents, especially against *B. subtilis* and *P. vulgaris*. The DFT calculations were performed to estimate its geometric structure and electronic properties. In addition, the most active pyridinone and pyrazole derivatives were further evaluated for in silico physicochemical, drug-likeness, and toxicity prediction. These derivatives obeyed all Lipinski's and Veber's rules without any violation and displayed non-immunotoxin, non-mutagenic, and non-cytotoxic. Molecular docking simulation was performed inside the active site of Topoisomerase IV (PDB:3FV5). It displayed binding energy ranging from -14.97 kcal/mol to -18.86 kcal/mol with hydrogen bonding and arene–cation interaction. Therefore, these derivatives were suggested to be good antibacterial agents via topoisomerase IV inhibitor.
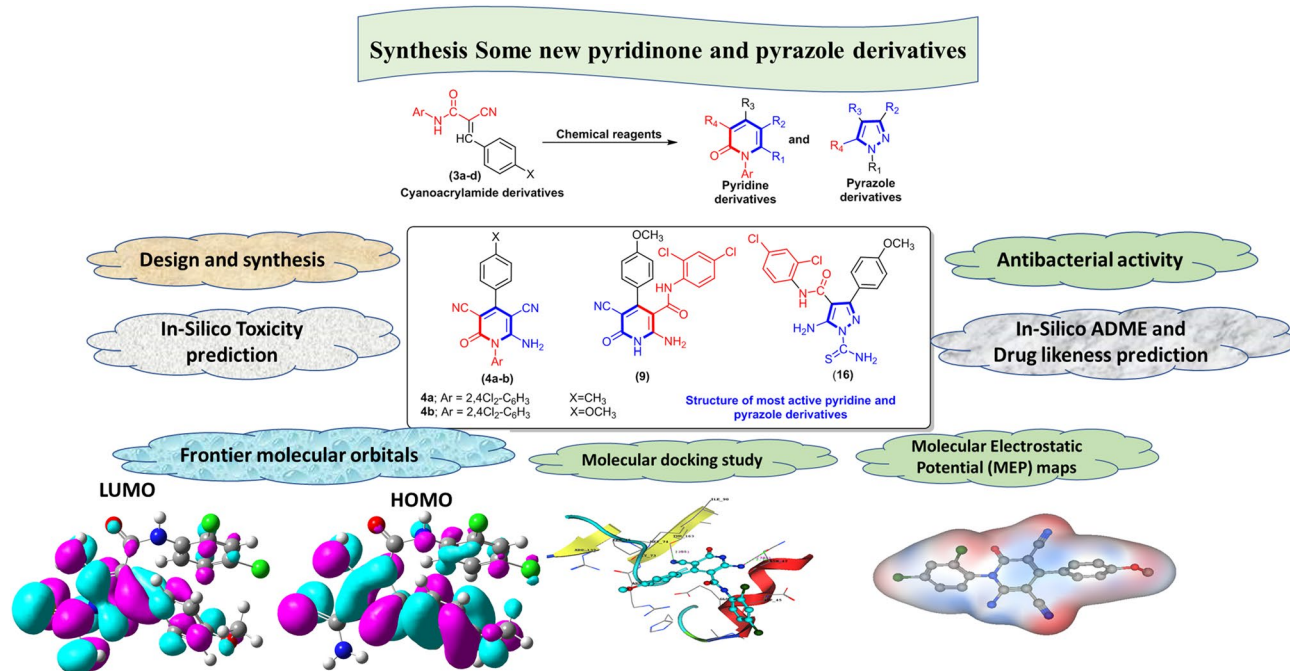
✉ Gameel A. M. Elhagali
   elhag1970@yahoo.com; elhag1970@azhar.edu.eg

✉ Ahmed Ragab
   ahmed_ragab@azhar.edu.eg; ahmed_ragab7@ymail.com

1 Department of Chemistry, Faculty of Science (Girls), Al-Azhar University, Nasr City, Cairo 11754, Egypt

2 Department of Chemistry, Faculty of Science (Boys), Al-Azhar University, Nasr City, Cairo 11884, Egypt

Graphical abstract

Keywords Cyanoacrylamide derivative · Pyridinone · Pyrazole · Antibacterial activity · DFT study · In silico ADME and toxicity prediction · Molecular docking
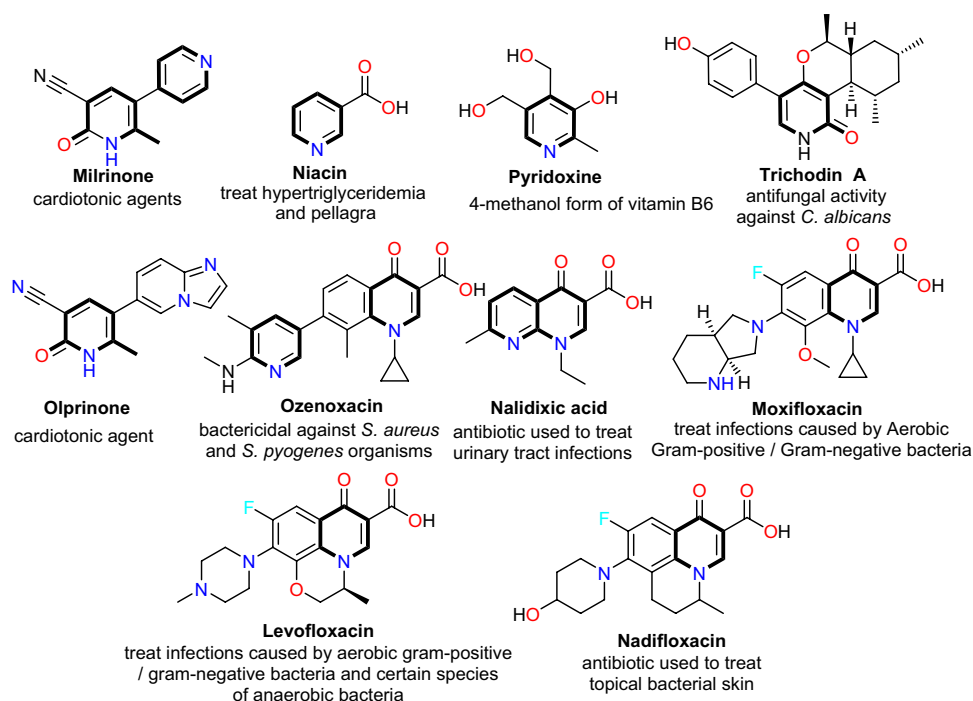
Introduction

Bacterial infections, which are caused by gram-positive and gram-negative pathogens, are responsible for the majority of hospital-acquired infections and lead to extensive mortality and burden on global healthcare systems [1, 2]. The emergency and widespread of drug-resistant organisms such as methicillin-resistant *S. aureus* (MRSA), methicillin-resistant *S. epidermidis* (MRSE), vancomycin-resistant *S. aureus* (VRSA), extended-spectrum *β*-lactamase (ESBL)-producing *E. coli*, and drug-resistant TB (DR-TB) has already increased up to an alarming level in the recent decades and is associated with considerable mortality [3]. The cyanoacetamide derivative contains two electrophilic centers that appeared at the carbon of carbonyl and carbon of the cyanide group. In addition, it includes two nucleophile centers localized on NH of acetamide and methylene group [4]. The advantage of cyanoacetamide enables chemists to study its reaction with common reagents to form a variety of heterocyclic compounds with pharmacological applications [5].

Furthermore, pyridine (C_5H_5N), an aromatic heterocycle in which a ring shares π electrons, forms one continuous circle of electrons besides the alternate double bonds shared by every atom on the circle [6]. Pyridine rings are present in many natural products, including vitamins such as

vitamin B6 and niacin's, coenzymes like nicotinamide adenine dinucleotide (NAD), and alkaloids as trigonelline [7]. One role of pyridine in medicinal chemistry is to improve water solubility because of its weak basicity, therefore, lead to improved pH [8]. Over 7000 known medications contain pyridine as the main core [9]. Additionally, pyridine is one of the most widely used groups that is reported to have many biological activities, including antitubercular [10], anticancer [11], antiviral [12], and antimicrobial [13]. Besides, the 4-(phenylamino)thieno[2,3-*b*]pyridine derivatives showed inhibitory activity against Herpes simplex virus type 1 (HSV-1) [14]. Various drugs contain a pyridine nucleus as anti-malarial [15], antidiabetic [16], antioxidants [17], anti-inflammatory [18] cardiotonic (as Milrinone and Olprnone) [19], and anti-amoebic agents [20]. Recently, two pyridinone derivatives, as di-dymellamide A and Trichodin A isolated from marine-derived fungi, exhibited antibiotic activity against clinically relevant microorganism, *S. epidermidis*, with lower MIC values [21] (Fig. 1). Besides, the pyridine ring fused with benzene to form a quinoline nucleus that is reported as a broad-spectrum antibiotic that is active against both Gram-positive and Gram-negative bacteria as Moxifloxacin, Nadifloxacin, Levofloxacin, Ozenoxacin, and Nalidixic acid. These drugs were mostly demonstrated to be bactericidal and exerted their mode of action to inhibit

Fig. 1 Examples of drugs containing pyridine or pyridinone cores in the literature

Milrinone
cardiotonic agents

Niacin
treat hypertriglyceridemia
and pellagra

Pyridoxine
4-methanol form of vitamin B6

Trichodin A
antifungal activity
against *C. albicans*

Olprinone
cardiotonic agent

Ozenoxacin
bactericidal against *S. aureus*
and *S. pyogenes* organisms

Nalidixic acid
antibiotic used to treat
urinary tract infections

Moxifloxacin
treat infections caused by Aerobic
Gram-positive / Gram-negative bacteria

Levofloxacin
treat infections caused by aerobic gram-positive
/ gram-negative bacteria and certain species
of anaerobic bacteria

Nadifloxacin
antibiotic used to treat
topical bacterial skin

the bacterial DNA replication or interfere with the synthesis of RNA and, consequently, with protein synthesis [22–24] (Fig. 1).

On the other hand, the pyrazole system is an important heterocyclic template, and its derivatives are rare in nature due to the difficulty of living organisms to construct N–N bond [25]. The pyrazole nucleus belonged to heterocycles aromatic compounds containing two adjacent nitrogen atoms in 1, 2 positions and therefore called 1,2 diazoles and have pharmacological effects on humans [26]. Also, pyrazole is used as a ligand for transition metal-catalyzed reactions [27] and is necessary as intermediates for synthesizing other pharmaceutical heterocycles [28–30]. The production of pyrazole and its derivatives showed various applications in the pharmaceutical and agriculture industries [31, 32]. It was reported that heterocycles containing pyrazole scaffold exhibit antibacterial [33] and anti-inflammatory[34], analgesic [35], antidepressant [36], antiviral [37], and antitumor activities [38]. Also, one of the important heterocycles that attracted good interest is the 5-aminopyrazole derivative used in a wide range of pharmaceutical applications [39].

Based on the previous literature and in continuous efforts to design and synthesize heterocyclic compounds that exhibited biological activities [40–44], the purpose of this work is to design and synthesize new pyridine or pyrazole derivatives from cyanoacrylamide derivatives. Additionally, the antibacterial activity screened against four bacterial strains. Moreover, the most active pyridinone and pyrazole derivatives were selected to determine the in silico physicochemical, drug-likeness, and toxicity prediction. The

DFT calculation was performed for exploring geometrical structural and reactivity parameters of the most actively studied compounds. Finally, the molecular docking simulation achieved to determine the binding mode and examine the compounds' interaction and binding activity inside the active site of Topoisomerase IV as the antimicrobial target.

Result and discussion

Chemistry

The synthesis of intermediate and the target compounds was outlined from Scheme 1 to Scheme 4 using cyanoacetamide derivatives as a starting material. The cyanoacetamide derivatives are highly reactive molecules and used as precursors or reaction intermediates because it contains two centers of reaction carbonyl and cyanocenters which make it able to react with widespread as bidentate reagents to form a variety of heterocycles [45, 46]. Our research is interested in the synthesis of pyridinone and pyrazole derivatives. According to the previously reported methods, the cyanoacetamide derivatives **1a,b** were prepared in a high yield [47, 48]. The cyanoacetamide derivatives **1a, b** and different aromatic aldehydes as *p*-methoxy benzaldehyde and *p*- tolualdehyde were heated under reflux condition in ethanol containing drops of piperidine gave the corresponding acrylamide derivatives **3a–d** (Scheme 1).

The structure of acrylamide derivatives **3a–d** approved using spectral analysis. The IR spectra of **3a–d** revealed
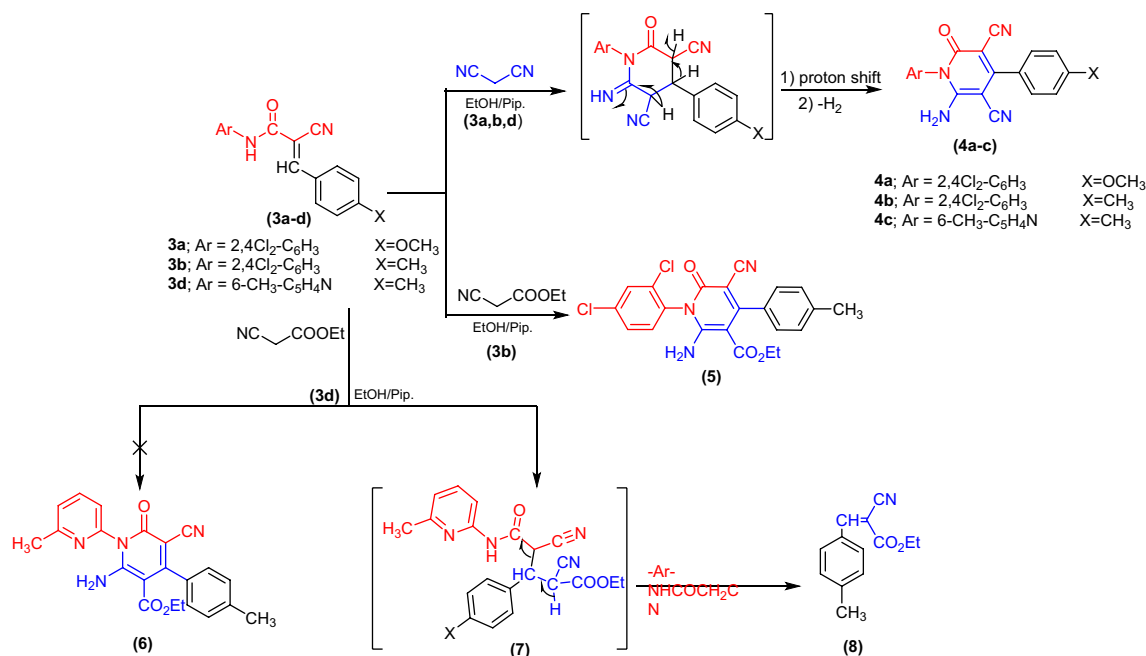
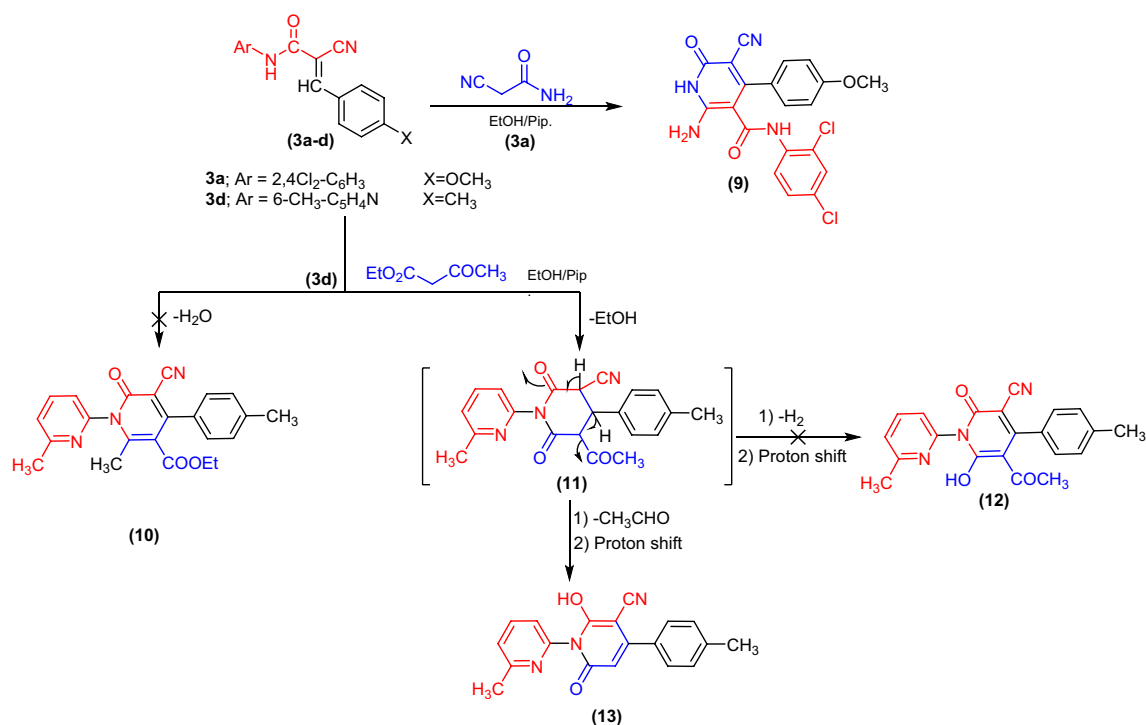**Scheme 1** Synthesis of acrylamide derivatives **3a–d**
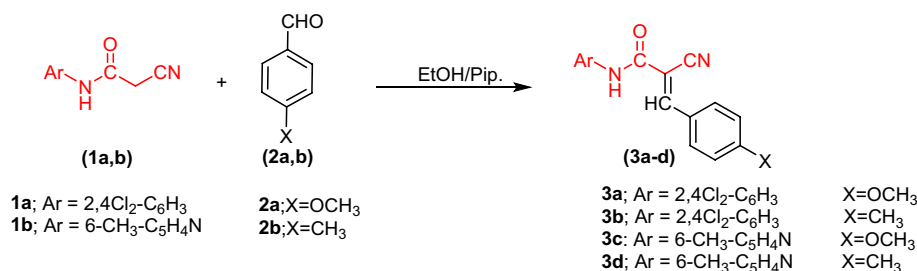
absorption bands for amidic carbonyl (1667–1696 cm⁻¹), cyano (2203–2217 cm⁻¹), and imino (3283–3397 cm⁻¹) groups at the correct frequencies. Additionally, the ¹H NMR spectrum of acrylamide derivative **3a** in (DMSO-d_6) displayed signals at δ 3.87 for methoxy group, and the aromatic protons at δ 7.13, 7.18, 7.49, 7.69, 7.27, and 8.06 ppm as five doublet signals with coupling constant ranged between (J = 8.4–9.0 Hz), and one singlet signal. Moreover, the acrylamide derivative **3a** displayed an exchangeable signal at δ 9.86 ppm related to the NH group and the methine proton (–CH=C–) appeared at δ 8.27 ppm. Its ¹³C NMR spectrum showed specific signals at δ 55.69, 151.56, and 163.03 ppm attributed to the methoxy, carbon attached to methoxy, and carbonyl group (C=O).

Cyclocondensation of acrylamide derivatives **3a**, **b**, **d** with malononitrile was afforded the corresponding 3,5-dicarbonitrile-2-oxo-pyridine **4a–c**. The mechanistic equation of this reaction can be described by attacking the active methylene (CH₂) to the carbanion β-carbon of acrylamide, then the NH nucleophile of cyanoacrylamide added to

the cyano-group of malononitrile, and then the cyclization occurred (Scheme 2). Spectral data and analytical analysis are in agreement with the postulated structure. The IR spectra showed stretching significance absorption bands for amino, cyano, and carbonyl groups at exact frequencies for **4a–c**. ¹H NMR spectrum (DMSO-d_6) revealed two singlet signals at δ 2.10, 2.32 ppm for two methyl protons, multiple signals between at δ 7.16 and 8.19 ppm due to seven aromatic protons, and exchangeable singlet signal at δ 6.66 ppm related to the amino group (NH₂) for pyridin-2-one derivative **4c**. Similarly, pyridine-2-one derivative **4a** appeared specific signal at δ 3.86 ppm, which referred to the methoxy group (OCH₃) due to exposure to ¹H NMR (DMSO-d_6). The fragmentation pattern of pyridine-2-one derivative **4a** is illustrated in chart S1.

Furthermore, refluxing of acrylamide derivatives **3b** and **3d** with ethyl cyanoacetate in ethanol catalyzed with piperidine (3drops) produced ethyl 2-amino-5-cyano-6-oxo-4-(4-methylphenyl)-pyridine-3-carboxylate derivative **5** and ethyl 2-cyano-3-(4-methylphenyl)acrylate derivative **8** [49]

Scheme 2 Synthesis of 3,5-dicyano-pyridine-2-one derivatives **4a–c** and 2-amino-6-cyanopyridin-6-one derivative **5**

Scheme 3 Synthesis 6-oxo-pyridine-3-carboxamide derivative **9** and 6-hydroxy2-oxo-4-(*p*-tolyl)-2*H*-[1,2'-bipyridine]-5-carbonitrile derivatives **13** based on cyanoacrylamide derivatives

rather than pyridine-2-one derivative **6**, respectively. The mechanistic route for formation of compound **8** represented as in Scheme 2.

The structure of 5-cyano-4-(4-methylphenyl)-pyridin-6-one derivative **5** was confirmed the result of spectral analyses. The ^{1}H NMR spectrum (DMSO-d_6) showed characteristic signals at δ 2.31, 1.51, 3.96 ppm corresponding to methyl and ethoxy group, besides signals between δ 7.22 and 7.64 ppm as three doublet and one singlet signals related seven aromatic protons and broad exchangeable signal at δ 7.26 ppm owning to the amino group (NH$_2$). Moreover, the ^{13}CNMR spectrum (DMSO-d_6) assigned signals at δ 1.67.61, 158.35, 155.16 ppm related to two carbonyl groups (2C=O) and carbon attached to the amino group (C-NH$_2$). Besides, three significant signals at δ 69.85, 20.95, and 29.05 ppm were assigned to the ethoxy and methyl groups, respectively.

The reaction of cyanoacrylamide derivative **3a** and cyanoacetamide derivative in one molar ratio under reflux condition in ethanolic piperidine afforded the corresponding 2-amino-5-cyano-6-oxo-pyridine-3-carboxamide derivative **9**. The IR spectrum displayed characteristic absorption bands at υ 3448, 3303, 3174, 2206, and 1697 cm^{-1} corresponding to NH, amino group (NH$_2$), nitrile (CN), and carbonyl (C=O) groups, respectively. The ^{1}H NMR spectrum of 6-oxo-pyridine-3-carboxamide derivative **9** revealed three significant exchangeable signals at δ 7.77, 7.83, and

7.96 ppm corresponding to amino and two NH groups. Besides, signals at δ 3.84 ppm for the methoxy group and the seven aromatic protons that ranging between δ 7.13 and 8.11 ppm. Additionally, the ^{13}C NMR spectrum displayed characteristic signals at δ 163.13, 162.56, 150.16, and 55.60 ppm for two carbonyl carbons (2C=O), carbon attached to the amino (C-NH$_2$), and methoxy (OCH$_3$) groups. The mass spectra showed a molecular ion peak at m/z=428.95 with an intensity of 25.52% corresponding to the molecular formula C$_{20}$H$_{14}$Cl$_2$N$_4$O$_3$ (Scheme 3).

Subsequent, reaction of cyanoacrylamide derivative **3d** with ethyl acetoacetate in absolute ethanol and in the presence of catalytic amount of piperidine (3 drops) afforded the corresponding 6-hydroxy-2-oxo-4-(*p*-tolyl)-2*H*-[1,2'-bipyridine]-5-carbonitrile derivative **13** rather than 5-acetyl-6-hydroxy-2-oxo-4-(*p*-tolyl)-2*H*-[1,2'-bipyridine]-3-carbonitrile derivative **12** and 3-cyano-2-oxo-4-(*p*-tolyl)-2*H*-[1,2'-bipyridine]-5-carboxylate derivative **10** based on the spectral data and elemental analysis. As described in Scheme 3, this reaction can be proceeded via two pathways: first one, elimination of water molecule to afford 2*H*-[1,2'-bipyridine]-5-carboxylate derivative **10**, while the second pathway, proceed via elimination of ethanol molecule to afford the intermediate **11**. The spectra data based on ^{1}H NMR spectra confirmed formation of compound **13**. The ^{1}H NMR spectra displayed significant two methyl groups at δ 2.37 and 2.43 ppm, singlet signal at δ 8.35 ppm related
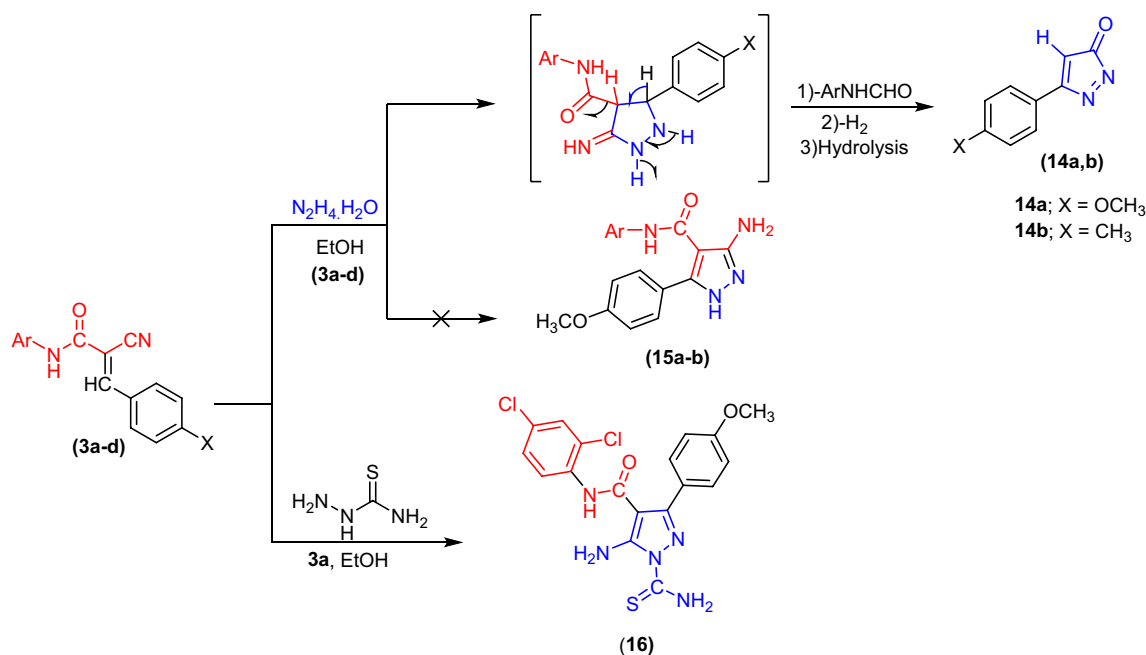
Scheme 4 Illustrates synthesis of new pyrazole derivatives **14a**, **b**, and **16** from the reaction of cyanoacrylamide derivatives **3a–d** with *bi*-nucleophile reagents as hydrazine hydrate and thiosemicarbazide

to pyridine-H, and one exchangeable singlet signal at δ 10.63 ppm assigned to the hydroxyl group. Additionally, the ^{13}C NMR spectrum exhibited signals at δ 161.22, 156.73, 151.14, 105.49, 23.51, and 21.25 ppm assignable to carbon attached to hydroxy group (C–OH), carbonyl group, C=N, and pyridine-C3, and two methyl groups, respectively. Besides, the mass spectra revealed a molecular ion peak at m/z = 317.72 with an intensity of 20.61% and related to empirical formula $C_{19}H_{15}N_3O_2$.

Here, the authors aimed to synthesize pyrazole nucleus from cyanoacrylamide derivatives hoping to add pyrazole nucleus that exhibit a versatile range of biological activities such as antimicrobial [50, 51], antidepressant [52], anti-inflammatory [34], antiviral [53], and antitumor activities [38]. Upon treatment, the acrylamide derivatives **3a–d** with hydrazine hydrate and thiosemicarbazide in ethanolic solution afforded the corresponding pyrazole derivatives **14a**, **b** and **16**, respectively (Scheme 4). The structure of pyrazole derivatives is confirmed with the usual spectroscopic techniques and elemental analysis. The IR spectra of pyrazole derivatives **14a**, **b** displayed a lack of significant amino group band and strong stretching frequency for carbonyl group at υ 1720 cm^{-1}. Additionally, the ^{1}H NMR spectra (DMSO-d_6) for the same compounds **14a, b** assigned specific signals for (OCH$_3$) and (CH$_3$) protons at δ 3.82 and 2.36 ppm, as well as the pyrazole protons at δ 8.62 for pyrazole derivative **14a**, and δ 8.55 ppm for pyrazole derivative **14b**. The fragmentation pattern of 5-(4-methoxyphenyl)-3H-pyrazol-3-one **14a** can be illustrated in chart S2.

Finally, the pyrazole derivative **16** showed new bands in the IR spectrum related to two amino groups at υ 3406, 3290, and 3151 cm^{-1}. Besides, the ^{1}H NMR spectrum showed singlet signal at δ 3.82 ppm of methoxy group, while three exchangeable signals appeared at δ 7.60, 7.89, and 11.33 ppm attributed to two amino (2NH$_2$) and one NH group, respectively. Besides, the seven aromatic protons ranging between δ 6.94–8.11 ppm. Also, ^{13}C NMR spectrum (DMSO–d_6) showed signals at δ 177.66, 160.72, 152.47, and 55.26 ppm attributed for thiocarbonyl (C=S), carbon attached to the methoxy (C-OMe), carbonyl group (C=O), and methoxy carbon (OCH$_3$), respectively.

Antibacterial activity with structure–activity relationship (SAR)

All the newly synthesized derivatives were evaluated for their in vitro antibacterial activity against two gram-positive strains as *S. aureus* (RCMB010010) and *B. subtilis* (RCMB 015), and two gram-negative strains as *E. coli* (RCMB010052) and *P. vulgaris* (RCMB004) by agar well diffusion method according to the previously reported methods [54–56]. The antibacterial activity is determined by the zone of inhibition expressed by (mm). Levofloxacin was used as positive control (Table 1). The preliminary assessment results exert varying activity against the tested bacteria pathogens. As can be seen in Table 1, the cyanoacrylamide derivatives **3a–d** showed no activity against *S. aureus* (RCMB010010) and *E. coli* (RCMB010052), while

Table 1 The antimicrobial activity represented by the zone of inhibition (IZ) mm for the newly synthesized acrylamide, pyridinone, and pyrazole derivatives, besides Gentamycin as the positive control

Exp Code	Gram-positive		Gram-negative	
	S. aureus (RCMB010010)	B. subtilis (RCMB 015)	E. coli (RCMB010052)	P. vulgaris (RCMB004)
3a	–	13.83 ± 0.15	–	17.13 ± 0.15
3b	–	11.20 ± 0.20	–	13.13 ± 0.012
3c	–	8.13 ± 0.15	–	8.03 ± 0.15
3d	–	8.10 ± 0.10	–	12.13 ± 0.12
4a	13.10 ± 0.10	12.13 ± 0.15	–	17.07 ± 0.12
4b	–	17.13 ± 0.15	9.17 ± 0.15	14.97 ± 0.25
4c	–	–	–	–
5				
9	11.07 ± 0.12	13.07 ± 0.12	–	18.07 ± 0.12
13	11.93 ± 0.21	–	–	14.90 ± 0.17
14a	10.17 ± 0.15	–	–	12.13 ± 0.15
14b	–	8.17 ± 0.15	7.97 ± 0.15	9.17 ± 0.21
16	14.93 ± 0.06	11.97 ± 0.15	–	16.87 ± 0.12
LEV	25.62 ± 0.31	21.18 ± 0.46	27.36 ± 0.45	26.52 ± 0.24

No activity (8 mm), weak activity (8–12 mm), moderate activity (12–15 mm), strong activity (>15 mm) and DMSO (solvent) (8 mm). Levofloxacin 4 µg/mL and the synthetized derivative 10 mg/mL

exhibited weak to good activity against *B. subtilis* (RCMB 015) and *P. vulgaris* (RCMB004).

Generally, the 2-cyano-*N*-(2,4-dichlorophenyl)acrylamide derivatives **3a, b** displayed moderate activity against *B. subtilis* with a zone of inhibition (IZ = 13.83 ± 0.15 and 11.20 ± 0.20) mm. Besides, the 3-(4-methoxyphenyl) acrylamide **3a** revealed the strongest activity against *P. vulgaris* with a zone of inhibition 17.13 ± 0.15 mm, while -3-(4-methylphenyl)acrylamide derivative **3b** showed moderate activity with inhibition zone 13.13 ± 0.012 mm. The higher activity of cyanoacrylamide derivative **3b** might be related to the presence of methoxy group that exhibited more effective than the methyl group in position three of 3-(aryl)-2-cyanoacrylamide derivatives **3a,b**.

On the contrary, 2-cyano-*N*-(6-methylpyridin-2-yl)acrylamide **3c**, **d** exhibited weak activity with the zone of inhibition ranged from 8.03 ± 0.15 to 12.13 ± 0.12 mm and changing the methyl by methoxy at aryl group in position three not enhancement the bacterial activity. This decrease in activity in acrylamide derivatives **3c, d** might be attributed to the replacement of *N*-(2,4-dichlorophenyl) with *N*-(6-methylpyridin-2-yl) moiety. Additionally, the 2-oxo-pyridine-3,5-dicarbonitrile **4a**, **b** showed moderate to potent activity against *S. aureus* and *P. vulgaris* with inhibition zones ranged between (12.13 ± 0.15–17.13 ± 0.15) mm and that might be attributed to the presence of two chlorine atoms in *N*-(2,4-dichlorophenyl) at position one in pyridine nucleus. Moreover, the 3,5-dicarbonitrile-1-(2,4-dichlorophenyl)-4-(4-methylphenyl)pyridine-2-one derivative **4b** displayed the highest activity compound against *B. subtilis* IZ = 17.13 ± 0.15 mm with an activity index of 80.87%

compared with Levofloxacin (IZ = 21.18 ± 0.45) mm, while it showed no activity against *S. aureus*. Additionally, the 2-cyano-*N*-(2,4-dichlorophenyl)acrylamide derivative **3a** and 3,5-dicarbonitrile-1-(2,4-dichlorophenyl)pyridine-2-one derivative **4b** demonstrated equipotent activity with the zone of inhibition 17 mm against *P. vulgaris*. Further, modification of pyridine-2-one derivatives **4a**, **b** to form bi-pyridine derivative **4c** in one hybrid structure causes a decrease in the antibacterial activity against all tested strains. Also, the 2-amino-5-cyano-6-oxo-pyridine-3-carboxylate derivative **5** exhibited no activity against the tested strains.

Surprisingly, the 2-amino-5-cyano-6-oxo-pyridine-3-carboxamide derivative **9** showed the most active derivatives against *P. vulgaris* with a zone of inhibition 18.07 ± 0.12 mm with an activity index nearly to 68% compared with Levofloxacin (IZ = 26.52 ± 0.24). This activity may be due to the presence of 3-carboxamide moiety at position three that bearing 2,4-dichlorophenyl group. Further, 6-oxo-pyridine-3-carboxamide derivative **9** revealed moderate activity against *B. subtilis* (IZ = 13.07 ± 0.12 mm) and weak activity against *S. aureus* (IZ = 11.07 ± 0.12 mm) in comparison to Levofloxacin (21.18 ± 0.46 and 25.62 ± 0.31) mm, respectively. The 6-hydroxy-2*H*-[1,2'-bipyridine]-5-carbonitrile derivative **13** demonstrated moderate activity against *P. vulgaris* (IZ = 14.90 ± 0.17) mm and *S. aureus* (IZ = 11.93 ± 0.21) mm, while displayed no activity against *B. subtilis* and *E. coli*. Notably, the 5-(Aryl)-3*H*-pyrazol-3-one derivatives **14a, b** exhibited weak activity against the tested strains and that might be due to absent of *N*-(2,4-dichlorophenyl) or pyridine moieties in their structure. Additionally, the 5-amino-1-carbamothioyl-1*H*-pyrazole-4-carboxamide

derivative **16** showed moderate to good activity against *B. subtilis* and *P. vulgaris* with an inhibition zone 11.97 ± 0.15, 16.87 ± 0.12 mm. respectively, and compared with Levofloxacin (IZ $= 21.18 \pm 0.46$ and 26.52 ± 0.24 mm). Besides, 1*H*-pyrazole-4-carboxamide derivative **16** revealed no activity against *E. coli* (RCMB010052) strains. However, the pyrazole derivative **16** showed moderate activity with zone of inhibition (14.93 ± 0.31 mm) against *S. aureus*, but still the highest antibacterial activity member in our study and that might be reflected to the combination between three pharmacophore groups as *N*-(2,4-dichlorophenyl) in the amide group, 4-methyl phenyl at C3 of pyrazole, and pyrazole moiety.

Finally, the preliminary assay results indicated that the most active derivatives **3a**, **4a**, **4b**, **9**, and **16** might lead to antibacterial agents, especially against *B. subtilis* and *P. vulgaris* and the SAR study can be summarized as;

(1) Presence of *N*-(2,4-dichlorophenyl) observed higher antibacterial activity than *N*-(6-methyl pyridine-2-yl) moiety as described in derivatives **3a–d**.

(2) For cyanoacrylamide derivative, the presence of methoxy at para position enhances the antibacterial activity than the methyl group.

(3) Formation of 6-aminopyridin-2-one derivatives **4a–c** improved the activity against *B. subtilis* and *P. vulgaris*, besides the presence of (4-methoxyphenyl) group in position four in pyridine-2-one derivative as **4a** causes inhibition to bacterial growth, especially against *S. aureus* strain.

(4) Adding the *N*-(2,4-dichlorophenyl) in the acetamide group as pyrazole derivative **16** improved the antibacterial activity against *S. aureus*, *B. subtilis*, and *P. vulgaris*

Computational and theoretical studies

Geometry optimization

Frontier molecular orbitals (FMOs) can be defined as highest occupied molecular orbitals (HOMO) and lowest unoccupied molecular orbitals (LUMO). The HOMO energy is an orbital that has ability of molecules to donate electrons, while LUMO energy represented the ability of molecule to revive electrons from occupied orbitals. The HOMO and LUMO orbitals are responsible for many molecular properties of molecules, including electronic properties, chemical reactivity, stability, a biological activity that is affected by intermolecular charge transfer [57, 58]. Based on the FMOs theory, it is believed that the antimicrobial properties of molecules are related to their LUMO energy, where molecules with low LUMO energy can accept more electron than those with high LUMO energy, which explains their higher activity [59]. A molecule with a high electron capacity may bind to protein more effectively because it interacts more effectively with the structure of the target protein [60]. The FMOs and chemical reactivity descriptors of the most active derivatives and Levofloxacin (positive control) are summarized in Table 2. Additionally, the pictorial drawing of HOMO–LUMO energies was shown in Fig. 2. Besides, The positive lopes are shown in turquoise color, whereas the negative phase is expressed in pale purple color.

Furthermore, the HOMO electron density of cyanoacrylamide derivative **3a** is localized over all the structure, while the LUMO is represented over the cyanoacrylamide except the 2,4-dichloro phenyl moiety. Additionally, the pyridine derivatives (**4a** and **4b**) of the HOMO and LUMO molecular orbital are distributed over the pyridine-2-one nucleus, except the 2,4-dichloro phenyl moiety. On the other hand, for the 2-amino pyridine-6-one derivative **9** the HOMO orbitals located in the bottom and left of the molecules around the pyridine nucleus and slightly distributed over the 4-tolyl group attached to position 4 in pyridine nucleus, while the LUMO orbital dispersed overall molecule. For 5-amino pyrazole derivative **16**, the HOMO and LUMO orbitals were

Table 2 Calculated chemical parameters of the most active derivatives and positive controls

Cpd No	E_{Total} (Hartree)	μ (Debye)	E_{HOMO} (eV)	E_{LUMO} (eV)	ΔE (eV)	IP (eV)	EA (eV)	X (eV)	η (eV)	S (eV^{-1})	μ_p (eV)	ω
3a	-1835.36	8.02	-6.25	-2.39	3.86	6.26	2.39	4.33	1.93	0.52	-4.33	4.84
4a	-1983.97	6.20	-6.17	-1.97	4.20	6.17	1.97	4.07	2.10	0.48	-4.07	3.94
4b	-2059.17	5.41	-6.08	-1.91	4.17	6.08	1.91	3.99	2.09	0.48	-3.99	3.82
9	-2135.64	5.22	-6.01	-1.82	4.18	6.01	1.82	3.92	2.09	0.48	-3.92	3.66
16	-2437.74	3.39	-5.86	-1.49	4.37	5.86	1.49	3.68	2.18	0.46	-3.68	3.09
LEV	-1262.96	10.21	-5.85	-1.65	4.19	5.85	1.65	3.75	2.09	0.48	-3.75	3.35

E_{Total} = Total energy (Hartree); μ = diploe moment (Debye); E_{HOMO} (eV); E_{LUMO} (eV); ΔE = energy bandgap (eV); IP = ionization potential; EA = electron affinity; X = electronegativity; η = chemical hardness; S = chemical softness; μ_p = chemical potential; ω = electrophilic index
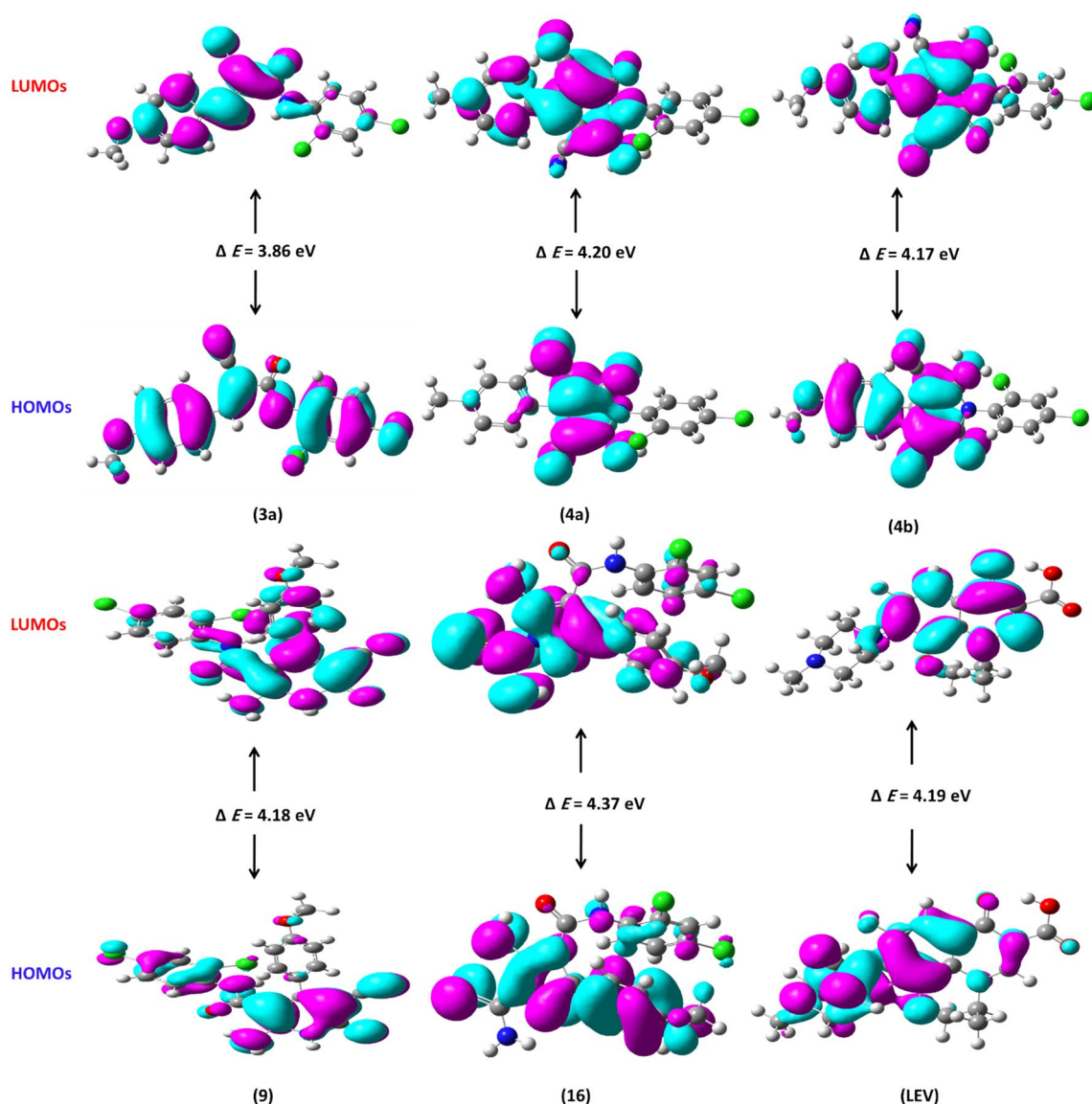
Fig. 2 Molecular orbital surfaces and energy bandgap of the most active derivatives and positive control

found to be localized over the pyrazole nucleus with a low density over the 4-methoxy phenyl group attached at position three in pyrazole. As a comparison, the HOMO orbital of Levofloxacin localized over the quinolone (benzo[b]pyridine) and piperazine derivatives. In contrast, the LUMO orbital was distributed over all molecule except the piperazine derivative.

As represented in Table (2), all the synthesized compounds displayed low total energy ranging from -1835.36 to -2437.74 Hartree compared to Levofloxacin ($E_{Total} = -1262.96$ Hartree). Besides, these derivatives showed dipole moment ranging between (3.39–8.02 Debye) compared with Levofloxacin ($\mu = 10.21$ Debye). Furthermore, the energy difference between HOMO and LUMO is the energy bandgap (ΔE) and reflects chemical stability. The

cyanoacrylamide derivatives **3a** showed the lowest energy bandgap $\Delta E = 3.86$ eV, while the pyrazole derivative **16** revealed the highest energy bandgap of 4.37 eV. Besides, the pyridine derivatives **4a**, **4b**, and **9** showed nearly equal energy bandgap ~ (4.17–4.20 eV) and were close to Levofloxacin ($\Delta E = 4.19$ eV). Moreover, the ionization potential can be defined as the energy required to remove an electron from a molecule's ground state.

On the other hand, electron affinity is represented by the energy released when a molecule in the ground state captures an electron. Additionally, in a chemical reaction, the hardness and the softness of a molecule are important descriptors. The synthesized derivatives exhibited high hardness and low softness values and were very close to Levofloxacin except for cyanoacrylamide derivative **3a**, which

displayed slightly harder and softer than the reset derivatives. Additionally, the electronegativity, chemical potential, and electrophilic index were calculated.

Furthermore, the electrophilicity (ω) is measured by the tendency of the molecule to accept an electron where the organic molecules can be classified as weak electrophiles (ω < 0.8), moderate electrophiles (ω = 0.8–1.5), and strong electrophiles (ω ˃ 1.5). The tested derivatives showed strong electrophilic properties with electrophilic index (ω) ranging between 3.09 and 4.84. the chemical potential (μp) indicates the probability of a chemical reaction occurring; a high value of (less negative) indicates that it is easier to donate electrons (electron donor), while a low value of (more negative) indicates that it is easier to accept electrons (electron acceptor). The synthesized derivatives demonstrated high chemical potential values. Thus, these derivatives are easy to donate an electron to the neighboring groups or biological target and could form different types of interaction inside the active site of the protein target.

In silico molecular docking study

Molecular docking simulation of the most active derivatives **3a**, **4a**, **4b**, **9**, and **16** was evaluated to determine the structure orientation, conformation and identify the binding mode of the most active derivatives inside the active site Topoisomerase IV (PDB:3FV5). The docking process was performed using Molecular operating Environmental (MOE) 10.2008, Chemical computing Group Inc, Montreal, Quench, Canada [61–63] according to the previously reported method [64]. The docking results are represented in Table S1 and Figs. 3, 4 and 5. The original ligand 1-(4-acetyl-6-pyridin-3-yl-1*H*-benzimidazol-2-yl)-3-ethylurea represented as **1EU** and displayed binding energy S = 23.60 kcal/mol with RMSD = 0.828 °A, through two hydrogen bonds sidechain donor between Asp69 and two NH of urea derivative with bond length 2.49 and 3.18 °A. Besides, one hydrogen bond

sidechain acceptor between the residue Arg132 and nitrogen of pyridine with bond length 3.09 °A and strength 13%, as well as one arene–cation interaction between Arg72 and pyridine nucleus is observed (the superimposition 3D of co-crystalized ligand and docking pose showed in Fig. 3). Additionally, the positive control used in antibacterial activity demonstrated binding energy S = − 20.72 kcal/mol. The Levofloxacin fitted inside the active site with two hydrogen bonds side chain donor between the Arg72 and carbonyl of carboxylic group of Levofloxacin with bond length 2.29 and 3.10 °A and strength 40 and 11%. Besides, the residue Asp69 bound with nitrogen of N-methyl piperazine with bond length 3.17 °A and strength 12% (See SI file).

Furthermore, cyanoacrylamide derivative **3a** showed binding energy S = − 14.97 kcal/mol, with binding mode, represented two hydrogen bond sidechain acceptors between Arg132 and Arg72 with the carbonyl of amide and nitrogen of cyano with bond length 2.83 and 3.08 °A, respectively. Besides, one arene–cation interaction between Arg132 and phenyl of 2,4-dichlorophenyl derivative is observed. Simultaneously, the pyridine-2-one derivative **4a** revealed only one hydrogen bond sidechain acceptor between the Arg132 and nitrogen of cyanide group with bond length 2.85 °A and strength 47%, as well as the tolyl group and dicyanide exhibited hydrophobic interaction. On the contrary, 3,5-dicarbo-nitrile-1-(2,4-dichlorophenyl)pyridine-2-one derivative **4b** showed one hydrogen bond sidechain donor between Glu46 and amino group localized at position six on pyridine-2-one derivative and arene cation interaction between phenyl of 2,4-dichlorophenyl (See SI file). Interestingly, 2-amino-5-cyano-6-oxo-pyridine-3-carboxamide derivative **9** revealed fitted inside the active site and showed the lowest binding energy S = − 18.86 kcal/mol through two sidechain hydrogen bonds: one hydrogen bond acceptor between Thr163 and nitrogen of cyanide and the other between Asn42 and amino group with bond length 3.02

Fig. 3 Shows the superimposition 3D of co-crystalized ligand (orange) and docking pose (green) with RMSD = 0.838 °A, inside the active site of topoisomerase IV (PDB:3FV5)
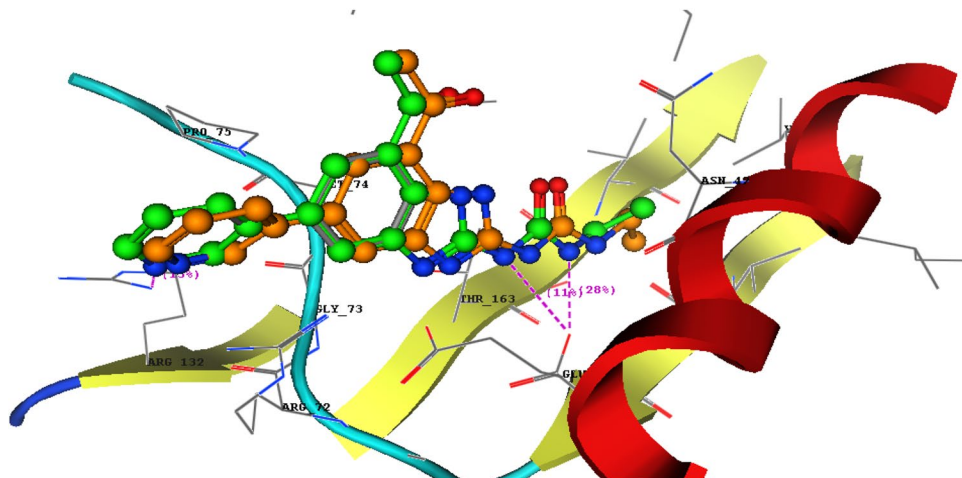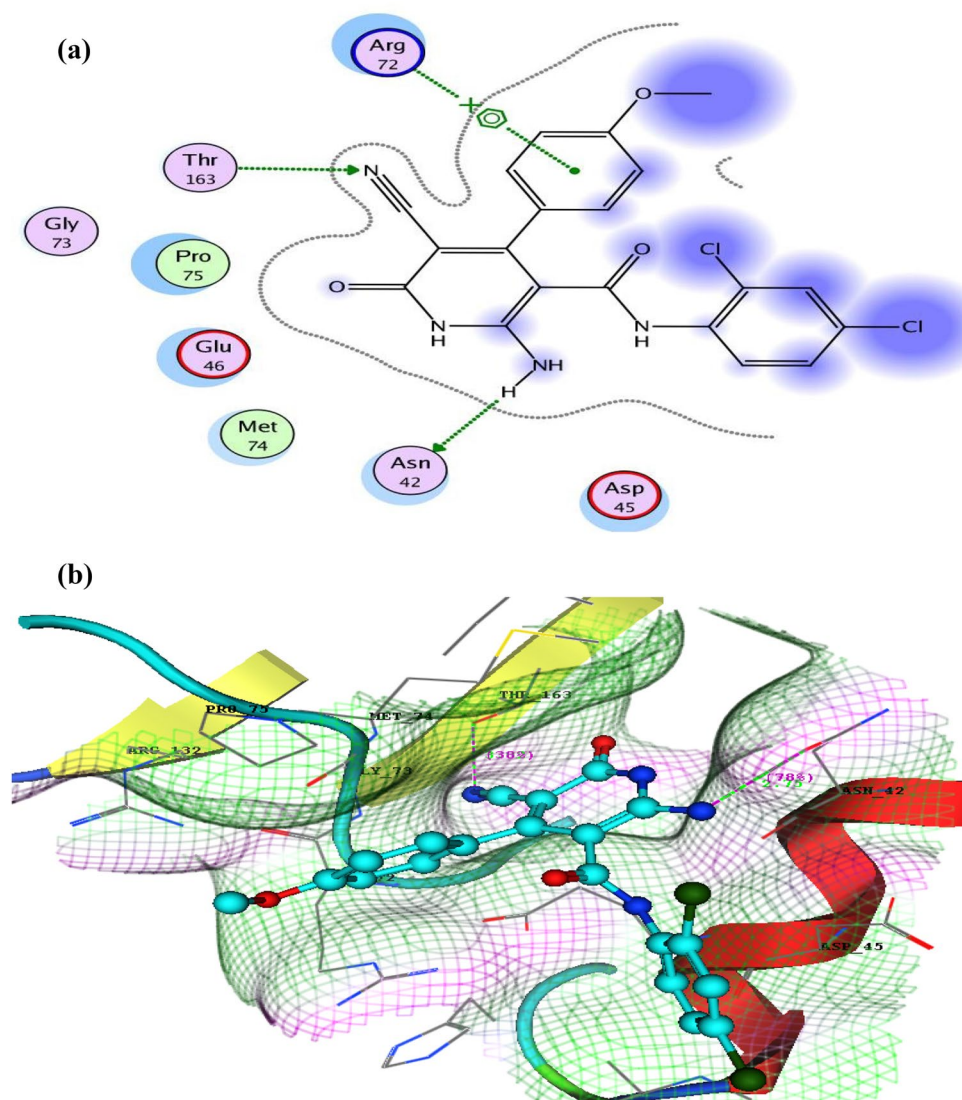
Fig. 4 **a** 2D structure of compound **9** inside the active site of topoisomerase IV (PDB:3FV5), **b** illustrated the 3D structure and mapping surface of the compound **9** inside the active site topoisomerase IV (PDB:3FV5)

and 2.75 °A, respectively. Besides, arene–cation interaction between the Arg72 and phenyl ring of the 4-methoxyphenyl group is observed (Fig. 4). Moreover, the 1-carbamothioyl-1*H*-pyrazole-4-carboxamide derivative **16** demonstrated one hydrogen bond sidechain donor between Arg132 and oxygen of methoxy group with bond length 3.07 and strength 21%, as well as two arene–cation interaction between Arg72 and pyrazole nucleus and Arg72 with phenyl of 4-methylphnyl group (Fig. 5).

Finally, it concluded that the most active derivatives could inhibit bacterial growth through topoisomerase IV inhibitors with binding energy ranging from − 14.97 to − 18.86 kcal/mol compared to co-crystallized ligand S = − 23.60 kcal/mol and Levofloxacin S = 20.72 kcal/mol. Additionally, all the most active derivatives exhibited at least one interaction as the co-crystallized ligand observed, and that showed the similarities in the structure of synthesized derivatives and co-crystallized ligand, and therefore, these derivatives were

suggested to be good antibacterial agents via topoisomerase IV inhibitor.

Molecular electrostatic potential (MEP) maps

MEP maps of a molecule are used to provide information about the positions of charge distribution (positive and negative charge) in the molecule and determine the active site for nucleophile and electrophile attack in the molecules for binding to protein in protein substrate interactions. The positive charge appears as blue color, and the negative charge appears as red color. Both of them can bind with the active site through different types of interaction (hydrogen bond donor, H-acceptor, arene–arene, and arene–cation interaction) and therefore confirmed the docking study. According to the previously reported method, the MEP was performed for the most active derivatives **3a**, **4a**, **4b**, **9**, **16,** and **Levofloxacin** using MOE 10.2008 [50]. As represented in Fig. 6,

Fig. 5 a 2D structure of compound **16** inside the active site of topoisomerase IV (PDB:3FV5), **b** illustrated the 3D structure and mapping surface of the compound **16** inside the active site topoisomerase IV (PDB:3FV5)
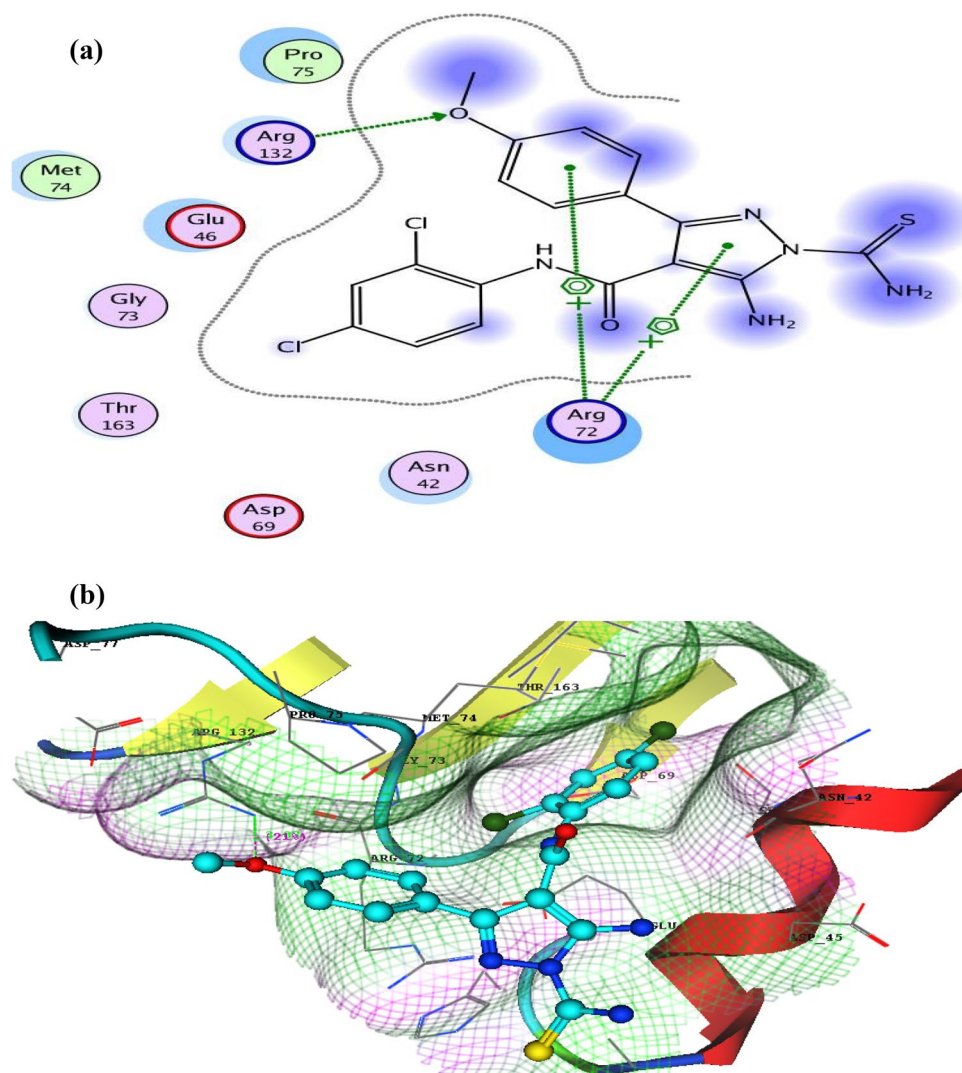
the positive charge was localized on NH of anilide derivative, amino of pyridine, the nitrogen of pyridine, amino at C5 of pyrazole, the nitrogen of pyrazole, amino of thioamide derivative, nitrogen of quinoline, and nitrogen of piperazine. On the other hand, the negative charge distributed around the nitrogen of cyano, oxygen of carbonyl at pyridinone, methoxy group, amide group, around chlorine atoms, sulfur of thioamide, and carboxylic group. Both the positive and negative charges are responsible for interaction between the ligand and active site in the docking study.

In silico ADMET study

The most active five derivatives **3a**, **4a**, **4b**, **9**, **16**, and Levo-floxacin were conducted to determine some physicochemical and drug-likeness properties, as well as the surface area represented by angstrom to estimate the drug-likeness of compounds using Molinspiration web tool according to the previously reported method [65, 66]. As shown in Table S2,

the most active derivatives **3a**, **4a**, **4b**, **9**, **16,** and Levofloxa-cin obeyed Lipinski's and Veber rule without any violation. Additionally, the most active derivatives have the number of hydrogen bond acceptor groups from four to seven and the number of hydrogen bond donors from one to five. Besides, topological polar surface area TPSA ranged between (62.12 and 121.01 $^{o}A^{2}$), molecular weight less than 500 Dalton, and partition coefficient MLogP from 3.64 to 4.59.

Subsequently, to determine the potential safety or toxicity of the most active derivatives **3a**, **4a**, **4b**, **9**, and **16** were assessed using two web tools as ProTox-II and pkCSM prediction as described previously [67, 68]. From Table S2, and based on ProTox-II prediction, the most active derivatives **3a**, **4a**, **4b**, and **16** belonged to class IV in toxicity classification with lethal dose LD_{50} ranged between 386 and 1000 mg/kg, while 6-oxo-pyridine-3-car-boxamide derivative **9** and Levofloxacin demonstrated $LD_{50} = 5000$ and 1478 mg/kg, respectively, and belongs to class V. Additionally, the most active derivatives and
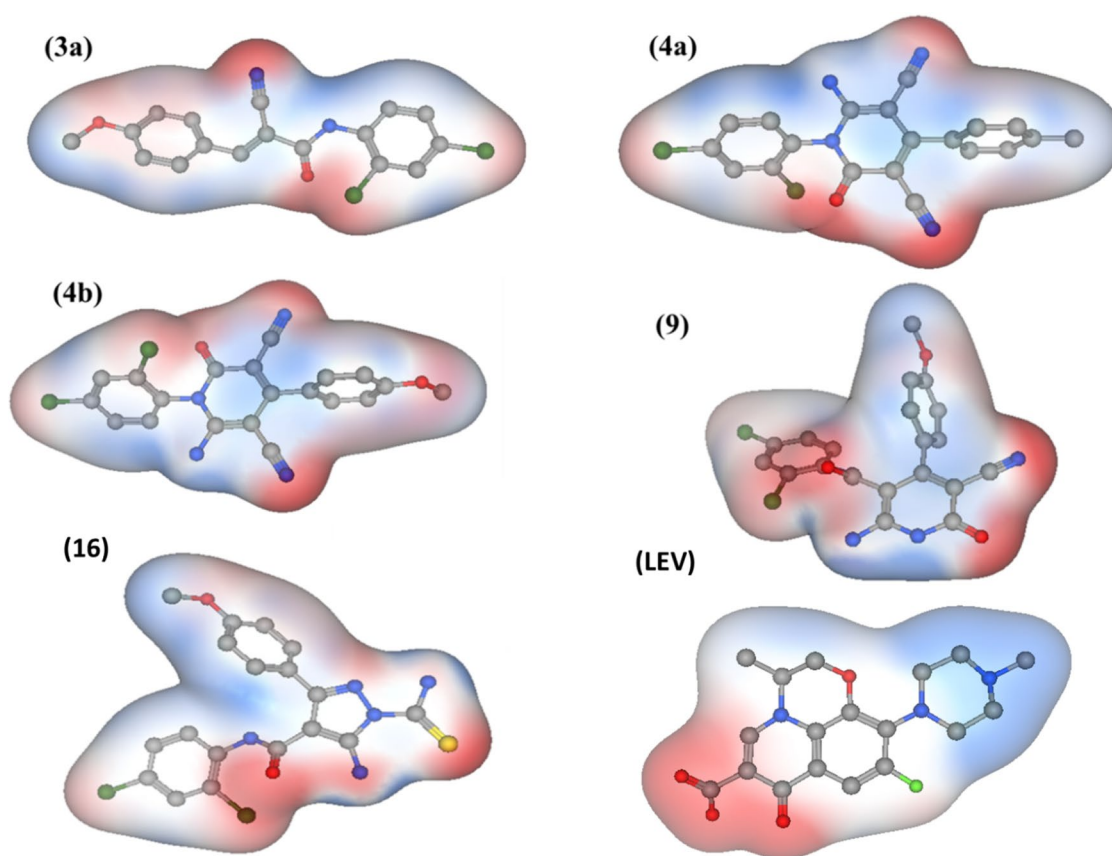
Fig. 6 shows the molecular electrostatic maps of the most active derivatives **3a**, **4a**, **4b**, **9**, **16,** and **Levofloxacin**, where the blue color indicates the positive charge and red color related to the negative charge

Levofloxacin displayed non-immunotoxin, non-mutagenic, and non-cytotoxic with probability ranged from 0.53 to 0.99, except cyanoacrylamide derivative **3a** and Levofloxacin that exhibited mutagenic with probability of 0.59 and 0.66, respectively.

Further, all the tested derivatives and positive control revealed inactive against phosphoprotein (Tumor suppressor) p53. Furthermore, the tested derivatives **3a**, **4a**, **4b**, **9**, and **16** showed non-hepatotoxic, non-skin sensitization, and no AMES toxicity, except pyridin-2-one **4a** that displayed a very low probability of AMES toxicity. Besides, the Levofloxacin and pyrazole derivative **16** predicted to have hepatotoxic properties. Moreover, the most active derivatives **3a**, **4a**, **4b**, **9**, **16**, and Levofloxacin showed no inhibition to hERG I, while **4a**, **4b**, **9**, **16** exhibited hERG II inhibitors. The tested compounds had max. tolerated doses (human) ranged from -0.026 to 0.446 (log mg/kg/day) lower than Levofloxacin 0.965 (log mg/kg/day). Besides, oral rat chronic toxicity (LOAEL) was predicted to have values ranging from 0.939 to 1.303 lower than Levofloxacin LOAEL = 1.79 (log mg/kg_bw/day). Similarly, the tested derivatives displayed oral rat chronic toxicity (LOAEL) between 2.576 and 2.775 mol/kg compared to Levofloxacin $LD_{50} = 2.59$ mol/kg.

Conclusion

The present study involves the synthesis and characterization of some new pyridinone and pyrazole derivatives based on cyanoacrylamide derivatives **3a–d** that were prepared previously by reaction of cyanoacetamide with different aldehydes. The synthesized compounds were assessed for their in vitro antibacterial activity by the agar well diffusion method and compared with Levofloxacin as a positive control. The preliminary assessment results exert varying activity against the tested bacteria pathogens from weak to good. Five derivatives **3a**, **4a**, **4b**, **9**, and **16** exhibited potent antibacterial activity with a zone of inhibition ranging from 11.07 ± 0.12 mm to 18.07 ± 0.12 mm and displayed the highest activity against *B. subtilis* and *P. vulgaris*. The most active derivatives **3a**, **4a**, **4b**, **9**, and **16** obeyed all rule of five and Veber's rule without any violation, and displayed non-immunotoxin, non-mutagenic, and non-cytotoxic.

Additionally, the most active derivatives **3a**, **4a**, **4b**, and **16** belonged to class IV in toxicity classification with lethal dose LD$_{50}$ ranged between 386 and 1000 mg/kg, while 6-oxo-pyridine derivative **9** demonstrated LD$_{50}$ = 5000 mg/kg belongs to class V. Surprisingly, the tested derivatives **3a**, **4a**, **4b**, **9**, and **16** showed non-hepatotoxic, non-skin sensitization, and no AMES toxicity, except pyridin-2-one **4a** that displayed a very low probability of AMES toxicity. Additionally, the pyrazole derivative **16** and Levofloxacin predictied to had hepatotoxic properties. Furthermore, the electronic parameters of the most active derivatives and Levofloxacin were analyzed by computing HOMO and LUMO orbitals. Additionally, quantum chemical parameters were evaluated and discussed using frontier molecular orbital analysis to explore the chemical reactivity of the most actives molecules. Finally, molecular docking simulation revealed that these derivatives suggested inhibiting bacterial growth through topoisomerase IV inhibitors with binding energy ranging from − 14.97 to − 18.86 kcal/mol compared to co-crystallized ligand S = -23.60 kcal/mol and Levofloxacin S = − 20.72 kcal/mol. Additionally, the MEP maps were studied to confirm the docking study by determining the position of groups that can bind with the possible sites involved in interactions with protein receptors.

Experimental

Chemistry

Melting points are uncorrected and recorded on digital Gallen Kamp MFB-595 instrument. The IR spectra were recorded on a Shimadzu 440 infrared spectrophotometer (v/cm^{-1}) using the KBr technique (Shimadzu, Japan). ^{1}H NMR spectra were recorded on a Varian Gemini spectrometer (δ/ppm) 300 MHz and Bruker spectrometer (400 MHz) spectrometer using trimethyl silane (TMS) as internal standard. The ^{13}C NMR spectra were run out at 75 MHz and ^{13}C NMR at (101 MHz, δ/ppm). Additionally, mass spectra were recorded on a Jeol-JMS-600 mass spectrometer. Further, the micro analytical data were obtained from the Micro analytical Research Centre, Faculty of Science, Cairo University. The reactions were monitored by thin layer chromatography (TLC) using TLC sheets with UV fluorescent silica gel Merck 60f254 plates using UV lamp and different solvents as mobile phases. The antimicrobial activity was evaluated at the Regional Center for Mycology and Biotechnology, Al-Azhar University. The 2-cyano-*N*-(2,4-dichlorophenyl) acetamide (**1a**) and 2-cyano-*N*-(6-methylpyridin-2-yl)acetamide (**1b**) were prepared using ethyl cyanoacetate according to the previously reported methods [47, 48].

Synthesis of 2-cyano-*N*-(aryl)-3-(aryl)acrylamide (3a–d).

To a solution cyanoacetamide derivative (**1a, b**) (0.01 mol) in absolute ethanol (20 mL) having little amount of piperidine (3drops), 4-methoxy benzaldehyde or 4-methylbenzaldehyde (0.01 mol) was added and heated under reflux for 3 h. The solid product formed was collected by filtration and recrystallized from ethanol.

2-Cyano-*N*-(2,4-dichlorophenyl)-3-(4-methoxyphenyl) acrylamide (3a)

Yellow powder (EtOH); Yield 72%; M.p. = 175–177 ºC; IR (KBr, v/cm^{-1}): 3283 (NH), 3078 (CH-arom.), 2939 (CH-aliph.), 2206 (C≡N) and 1697 (C=O amide) ^{1}H NMR (300 MHz DMSO-d_{6}): δ/ppm 3.87(s, 3H, OCH$_{3}$), 7.13 (d, 1H, J=8.7 Hz, Ar–H), 7.18 (d, 1H, J=9.0 Hz, Ar–H), 7.49 (d, 1H, J=8.4 Hz, Ar–H), 7.69 (d, 1H, J=8.7 Hz, Ar–H), 7.27 (s, 1H, A-H), 8.06 (d, 2H, J=8.7 Hz, Ar–H), 8.27 (s, 1H, methine-H), 9.86 (s, 1H, NH exchangeable by D$_{2}$O); ^{13}C NMR (76 MHz DMSO-d_{6}): δ/ppm 163.03 (C=O), 151.56 (C-Ome), 141.54 (C=C), 132.88, 131.79, 130.89, 130.18, 130.03, 129.73, 129.10, 128.48, 127.78, 124.21, 116.75, 114.95, 114.50, 55.69 (OMe); Anal. Calcd. for C$_{17}$H$_{12}$Cl$_{2}$N$_{2}$O$_{2}$ (346.03): C, 58.81; H, 3.48; N, 8.07; Found: C, 58.98; H, 3.28; N, 8.22.

2-Cyano-*N*-(2,4-dichlorophenyl)-3-(4-methylphenyl) acrylamide (3b)

Yellow powder (EtOH); Yield 72%; M.p. = 246–248 ºC; IR (KBr, v/cm^{-1}): 3339 (NH), 3050 (CH-arom.), 2980, 2836 (CH-aliph.), 2217 (C≡N), and 1667 (C=O amide); ^{1}H NMR (300 MHz DMSO-d_{6}): δ/ppm 2.49 (s, 3H, CH$_{3}$), 7.07 (d, 2H, J=7.8 Hz, Ar–H), 7.39 (d, 2H, J=8.7 Hz, Ar–H), 7.62 (s, 1H, Ar–H), 8.11 (d, 2H, J=8.7 Hz, Ar–H), 8.34 (s, 1H, methine-H), 9.13 (s, 1H, NH, exchangeable by D$_{2}$O); ^{13}C NMR (101 MHz, DMSO d_{6}) δ/ppm 163.97 (C=O), 151.91, 147.99, 143.98, 139.49, 135.93, 132.03, 130.03, 126.80, 125.44, 124.58, 121.19, 117.31 (Ar-Cs), 115.46 (CN), 102.66, 19.02 (CH$_{3}$); Anal. Calcd. for C$_{17}$H$_{12}$Cl$_{2}$N$_{2}$O (330.03): C, 61.65; H, 3.65; N, 8.46; Found: C, 61.92; H, 3.89; N, 8.12.

2-Cyano-3-(4-methoxyphenyl)-*N*-(6-methylpyridin-2-yl)acrylamide (3c)

Yellow powder (EtOH); Yield: 87%; M.p. = 190–192 ºC; IR (KBr, v/cm^{-1}): 3397 (NH), 3056 (CH-arom.), 2976, 2922 (CH-aliph.), 2206 (C≡N), and 1688 (C=O amide); ^{1}H NMR (300 MHz DMSO-d_{6}): δ/ppm 2.49 (s, 3H, CH$_{3}$), 3.87 (s, 3H, OCH$_{3}$), 7.06 (d, 1H, J=7.5 Hz, Ar–H), 7.18 (d, 2H, J=9.0 Hz, Ar–H), 7.76 (t, 1H, J=7.8 Hz, Ar–H), 7.89 (d, 1H, J=8.4 Hz, Ar–H), 8.03 (d, 2H, J=8.7 Hz, Ar–H), 8.31 (s, 1H,methine-H),10.55 (s, 1H, NH, exchangeable by D$_{2}$O); ^{13}C NMR (76 MHz DMSO-d_{6}): δ/ppm 162.83 (C=O), 161.47 (C-OMe), 156.79 (C=$\underline{C}$-N), 150.79 (C=N), 138.61, 132.71, 124.33, 119.40, 116.75, 114.84, 111.18, 103.12, 55.64 (OCH$_{3}$), 23.52 (CH$_{3}$); Anal. Calcd. for C$_{17}$H$_{15}$N$_{3}$O$_{2}$ (293.33): C, 69.61; H, 5.15; N, 14.33 Found: C, 69.32; H, 5.43, N, 14.07.

2-Cyano-3-(4-methylphenyl)-*N*-(6-methylpyridin-2-yl) acrylamide(3d)

Yellow powder (EtOH); Yield 85%; M.p. = 140–142 ºC; IR (KBr, ν/cm^{-1}): 3396 (NH), 3015 (CH-arom.), 2959, 2920 (CH-aliph.), 2203 (C≡N) and 1698 (C=O amide); ^{1}H NMR (300 MHz DMSO-d_6): δ/ppm 2.24, 2.49 (2 s, 6H, 2CH$_3$), 7.06 (d, 2H, J = 7.2 Hz, Ar–H), 7.42 (d, 2H, J = 8.4 Hz, Ar–H), 7.76 (t, 1H, Ar–H), 7.91 (d, 2H, J = 8.4 Hz, Ar–H), 8.32(s, 1H, methine-H),10.72 (s, 1H, NH exchangeable by D$_2$O); ^{13}C NMR (76 MHz DMSO-d_6): δ/ppm 161.27 (C=O), 158.05 (C=$\underline{C}$-N), 156.76 (C=N), 151.18 (C=$\underline{C}$H), 143.72, 138.96, 130.97, 129.32, 119.49, 116.37, 111.24, 106.11, 105.52, 23.71, 21.27 (2CH$_3$); Anal. Calcd. for C$_{17}$H$_{15}$N$_3$O (277.33): C, 73.63; H, 5.45; N, 15.15 Found: C, 73.31; H, 5.52, N, 14.97.

Synthesis of 6-amino-1-(aryl)-2-oxo-4-(aryl)-1,2-dihydropyridine-3,5-dicarbonitrile (4a–c)

To a solution of acrylamide derivatives **3a–d** (0.01 mol) in absolute ethanol (20 mL) catalyzed with piperidine (3drops), malononitrile (0.01 mol) was added. The reaction mixture was heated under reflux for 6 h. The solid products obtained were collected by filtration and recrystallized from ethanol.

6-Amino-1-(2,4-dichlorophenyl)-2-oxo-4-(4-methoxyphenyl)-1,2-dihydropyridine-3,5-dicarbonitrile (4a)

Brown crystals (EtOH); Yield: 77%; M.p. = 229–231 ºC; IR (KBr, ν/cm^{-1}): 3452, 3213, 3174 (NH$_2$), 3097 (CH-arom.), 2970, 2935 (CH-aliph.), 2225, 2202 (C≡N) and 1678 (C=O amide); ^{1}H NMR (400 MHz, DMSO-d_6) δ/ppm 3.81 (s, 3H, OCH$_3$), 6.77 (s, 2H, NH$_2$ exchangeable by D$_2$O), 6.90 (d, J = 7.6 Hz, 1H, Ar–H), 7.09 (d, J = 7.2 Hz, 1H, Ar–H), 7.26 (d, J = 7.6 Hz, 1H, Ar–H), 7.48 (s, 1H, Ar–H), 7.89 (d, J = 7.2 Hz, 2H, Ar–H); ^{13}C NMR (101 MHz, DMSO-d_6) δ/ppm 160.48 (C=O), 159.28 (C-NH$_2$), 157.80 (C-OMe), 156.63 (C=$\underline{C}$-Ar), 145.47, 135.90, 130.21, 129.45, 128.88, 127.33, 126.16, 116.23, 115.57, 113.80, 113.67 (2CN), 87.41, 75.04 (2$\underline{C}$-CN), 55.00 (OCH$_3$); Anal. Calcd. for C$_{20}$H$_{12}$Cl$_2$N$_4$O$_2$ (410.03): C, 58.41; H, 2.94; N, 13.62 Found: C, 58.73; H, 3.21, N,13.94.

6-Amino-1-(2,4-dichlorophenyl)-2-oxo-4-(4-methylphenyl)-1,2-dihydropyridine-3,5-dicarbonitrile (4b)

Pale brown crystals (EtOH); Yield 77%; M.p. = 242–244 ºC; IR (KBr, ν/cm^{-1}): 3485, 3421 (NH$_2$), 3087 (CH-arom.), 2982 (CH-aliph.), 2218, 2209 (C≡N), and 1650 (C=O amide); ^{1}H NMR (400 MHz, DMSO-d_6) δ/ppm 2.18 (s, 3H, CH$_3$), 6.75 (s, 2H, NH$_2$, exchangeable by D$_2$O), 7.48 (d, J = 8.0 Hz, 2H, Ar–H), 7.53 (d, J = 8.4 Hz, 2H, Ar–H), 7.63 (d, J = 8.4 Hz, 2H, Ar–H), 7.91 (s, 1H, Ar–H); ^{13}C NMR (101 MHz, DMSO-d_6) δ/ppm 161.88 (C=O), 159.04 (C-NH$_2$), 157.69 (C=$\underline{C}$-Ar), 145.36, 135.78, 134.71, 133.09, 130.72, 130.46, 129.46, 128.73, 128.43, 127.92,

127.83, 127.24, 115.82, 115.18 (2CN), 87.16, 75.16 (2$\underline{C}$-CN), 21.81 (CH$_3$); MS m/z (%): 395.67 (M$^+$, 20.12), 343.84 (100%); Anal. Calcd. for C$_{20}$H$_{12}$Cl$_2$N$_4$O (395.24): C, 60.78; H, 3.06; N, 14.18 Found: C, 60.32; H, 3.41, N, 14.45.

6-Amino-6'-methyl-2-oxo-4-(4-methylphenyl)-2*H*-[1,2'-bipyridine]-3,5-dicarbonitrile (4c)

Brown crystals (EtOH); Yield: 69%; M.p. = 225–227 ºC; IR (KBr, ν/cm^{-1}): 3305, 3213 (NH$_2$), 3035 (CH-arom.), 2981, 2931 (CH-aliph.), 2218, 2191 (2C≡N), and 1647 (C=O amide); ^{1}H NMR (400 MHz, DMSO-d_6) δ/ppm 2.10, 2.32 (2 s, 6H, 2CH$_3$), 6.66 (s, 2H, NH$_2$ exchangeable by D$_2$O), 7.16 (d, J = 6.8 Hz, 2H, Ar–H), 7.79–7.68 (m, 2H, Ar–H), 8.00 (d, J = 6.8 Hz, 2H, Ar–H), 8.19 (t, 1H, Ar–H); ^{13}C NMR (101 MHz, DMSO-d_6) δ/ppm 160.78 (C=O), 157.52 (C–NH$_2$), 150.37 (C = $\underline{C}$–Ar), 140.26, 139.18, 132.19, 131.07, 129.22, 125.97, 123.73, 121.67, 119.42, 115.08, 114.41 (2CN), 85.36, 79.13 (2$\underline{C}$-CN), 24.68, 21.43 (2CH$_3$); Anal. Calcd. for C$_{20}$H$_{15}$N$_5$O (341.37): C, 70.37; H, 4.43; N, 20.52; Found: C, 70.21; H, 4.77, N, 20.78.

Ethyl 2-amino-5-cyano-1-(2,4-dichlorophenyl)-6-oxo-4-(4-methylphenyl)-1,6-dihydropyridine-3-carboxylate (5)

A mixture of acrylamide derivative **3b** (0.01 mol) in absolute ethanol (20 mL) catalyzed with piperidine (3 drops) and ethyl cyanoacetate (0.01 mol) was heated under reflux for 6 h. The solid product obtained was collected by filtration and recrystallized from ethanol.

White crystals (EtOH); Yield 59%; M.p. = 200–202 ºC; IR (KBr, ν/cm^{-1}): 3383, 3278 (NH$_2$), 3066 (CH-arom.), 2993 (CH-aliph.), 2206 (C≡N) and 1639 (br C=O amide); ^{1}H NMR (300 MHz DMSO-d_6): δ/ppm 1.51 (t, 3H, CH$_3$), 2.31 (s, 3H, CH$_3$), 4.23 (q, 2H, J = 7.7 Hz, CH$_2$), 7.22 (d, 2H, J = 7.5 Hz, Ar–H), 7.26 (s, 2H, NH$_2$ exchangeable by D$_2$O), 7.33 (d, 2H, J = 8.1 Hz, Ar–H), 7.49 (d, 1H, Ar–H), 7.55 (d, 1H, Ar–H), 7.64 (s, 1H, Ar–H); ^{13}C NMR (75 MHz DMSO-d_6): δ/ppm 167.61, 158.35 (C=O), 155.16 (C-NH$_2$), 137.95, 136.35, 134.24, 130.70, 129.13, 128.82, 128.17, 128.26, 127.98, 127.76, 127.38, 125.15, 100.79, 69.58 (O-$\underline{CH_2}$CH$_3$), 29.05 (CH$_3$), 20.95 (O-CH$_2\underline{CH_3}$); MS m/z (%): 442.86 (M$^+$, 6.21), 286.38 (100%); Anal. Calcd. for C$_{22}$H$_{17}$Cl$_2$N$_3$O3 (442.30): C, 59.74; H, 3.87; N, 9.50 Found: C, 59.34; H, 3.33, N, 9.81.

2-Amino-5-cyano-*N*-(2,4-dichlorophenyl)-4-(4-methoxyphenyl)-6-oxo-1,6-dihydropyridine-3-carboxamide (9)

A solution of acrylamide derivatives **3a** (0.01 mol) in absolute ethanol (20 mL) catalyzed with piperidine (3 drops) was heated under reflux condition with cyan acetamide (0.01 mol) for 7 h. The solid product obtained was collected by filtration and recrystallized from ethanol.

Pale orange (EtOH); Yield 71%; M.p. = 198–200 ºC; IR (KBr, ν/cm^{-1}): 3448, 3303, 3174 (NH$_2$, NH), 3043 (CH-arom.), 2961, 2908 (CH-aliph.), 2206 (C≡N) and 1697

(C=O amide); ^{1}H NMR (300 MHz DMSO-d_6): δ/ppm 3.84 (s, 3H, OCH$_3$), 7.13 (d, 2H, Ar–H), 7.32 (d, 1H, Ar–H), 7.51 (d, 2H, Ar–H), 7.77 (s, 2H, NH$_2$ exchangeable by D$_2$O), 7.83 (s, 1H, NH exchangeable by D$_2$O), 7.88 (d, 1H, Ar–H), 7.96 (s, 1H, NH exchangeable by D$_2$O), 8.11 (s, 1H, Ar–H); ^{13}C NMR (76 MHz DMSO-d_6): δ/ppm 163.13, 162.56 (2C=O), 150.16 (C-NH$_2$), 144.65 (C=C), 142.95, 132.45, 128.64, 126.34, 124.40, 120.47, 117.09, 114.88, 112.54, 102.90, 55.60 (OCH$_3$); MS m/z (%): 428.95 (M$^+$, 25.52). Anal. Calcd. for C$_{20}$H$_{14}$Cl$_2$N$_4$O$_3$ (428.04): C, 55.69; H, 3.29, N, 13.05. Found: C, 55.84; H, 3.53, N, 12.84.

6-Hydroxy-6'-methyl-2-oxo-4-(4-methylphenyl)-2H-[1,2'-bipyridine]-5-carbonitrile (13).

A mixture of acrylamide derivatives 3d (0.01 mol) in absolute ethanol (20 mL) catalyzed with piperidine (3 drops) and ethyl acetoacetate (0.01 mol) was heated under reflux for 6 h. The solid product obtained was collected by filtration and recrystallized from ethanol.

Pale orange (EtOH); Yield 73%; M.p. = 165–167 ºC; IR (KBr, ν/cm^{-1}): 3402 (OH), 3008 (CH-arom.), 2966 (CH-aliph.), 2206 (C≡N), and 1693 (C=O amide); ^{1}H NMR (300 MHz DMSO-d_6): δ/ppm 2.37, 2.43 (2 s, 6H, 2CH$_3$), 7.03 (d, 1H, J = 7.5 Hz, Ar–H), 7.38 (d, 2H, J = 7.8 Hz, Ar–H), 7.68 (s, 1H, Ar–H), 7.73 (d, 1H, J = 7.8 Hz, Ar–H), 7.89 (d, 2H, J = 8.1 Hz, Ar–H), 8.35 (s, 1H, pyridine-H), 10.62 (s, 1H, OH; exchangeable by D$_2$O); ^{13}C NMR (76 MHz DMSO-d_6): δ/ ppm 161.22 (C–OH), 156.73 (C=O), 151.14 (C=N), 150.74 (C=C-Ar), 143.25, 138.58, 130.31, 129.82, 129.14, 119.46, 116.35, 111.22, 105.49, 23.51 (CH$_3$), 21.25 (CH$_3$); MS m/z (%): 317.72 (M$^+$, 20.61), 137.39 (100%); Anal. Calcd. For C$_{19}$H$_{15}$N$_3$O$_2$ (317.35): C, 71.91; H, 4.76, N, 13.24. Found: C, 71.62; H, 4.32; N, 12.95.

Synthesis of 5-(Aryl)-3H-pyrazol-3-one (14a,b)

To a solution of acrylamide derivatives 3a–d (0.01 mol) in absolute ethanol (20 mL), hydrazine hydrate (0.01 mol) was added and the reaction mixture was heated under reflux for 3–5 h. The solid products obtained were collected by filtration and recrystallized from ethanol.

5-(4-Methoxyphenyl)-3H-pyrazol-3-one (14a)

Yellow powder (EtOH); Yield 66%; M.p. = 165–167 ºC; IR (KBr, ν/cm^{-1}): 3062 (CH-arom.), 2970 (CH-aliph.), and 1660 (C=O amide) ^{1}H NMR (300 MHz DMSO-d_6): δ/ppm 3.82 (s, 3H, OCH$_3$), 7.55 (d, 2H, Ar–H), 7.82 (d, 2H, Ar–H), 8.62 (s, 1H, Pyrazole-H); ^{13}C NMR (76 MHz DMSO-d_6): δ/ppm 161.66 (C=O), 160.50 (C-OMe), 129.96, 126.55, 114.39, 55.36 (C-OMe); MS m/z (%): 188.04 (M$^+$, 38.72), 185.86 (100%); Anal. Calcd. For C$_{10}$H$_8$ N$_2$O$_2$ (188.19): C, 63.83; H, 4.29, N; 14.89. Found: C, 63.52; H, 3.687; N, 14.65.

5-(4-Methylphenyl)-3H-pyrazol-3-one (14b)

Brown powder (EtOH); Yield 69%; M.p. = 150–152 ºC; IR (KBr, ν/cm^{-1}): 3062 (CH-arom.), 2970 (CH-aliph.), and 1655 (C=O amide); ^{1}H NMR (300 MHz DMSO-d_6): δ/ ppm 2.36 (s, 3H, CH$_3$), 7.32 (d, 2H, J = 8.1 Hz, Ar–H), 7.77 (d, 2H, J = 7.8 Hz, Ar–H), 8.55 (s, 1H, pyrazole-H); ^{13}C NMR (76 MHz DMSO-d_6): δ/ppm 161.24 (C=O), 141.32, 131.19, 129.51, 128.31, 21.51 (CH$_3$); MS m/z (%): 172.02 (M$^+$, 42.54), 69.09 (100%); Anal. Calcd. For C$_{10}$H$_8$ N$_2$O (172.19): C, 69.77; H, 4.68, N; 16.27. Found: C,70.23; H, 4.22; N, 16.54.

5-Amino-1-carbamothioyl-N-(2,4-dichlorophenyl)-3-(4-methoxyphenyl)-1H-pyrazole-4-carboxamide (16).

A mixture of acrylamide derivative 3b (0.01 mol) in absolute ethanol (20 mL) and thiosemicarbazide (0.01 mol) was heated under reflux for 6 h. The solid product obtained was collected by filtration and recrystallized from ethanol.

Pale brown crystals (EtOH); Yield 78%; M.p. = 150–152 ºC; IR (KBr, ν/cm^{-1}): 3406, 3290, 3151 (NH, NH$_2$), 3041 (CH-arom.), 2970 (CH-aliph.), and 1651 (C=O amide); ^{1}H NMR (300 MHz DMSO-d_6): δ/ppm 3.82 (s, 3H, OCH$_3$), 6.94 (d, 2H, J = 6.9 Hz, Ar–H), 7.01 (d, 2H, J = 8.1 Hz, Ar–H), 7.60 (s, 2H, NH$_2$ exchangeable by D$_2$O), 7.73 (d, 1H, J = 6.9 Hz, Ar–H), 7.89 (s, 2H, NH$_2$ exchangeable by D$_2$O), 8.03 (d, 1H, Ar–H), 8.11 (s, 1H, Ar–H), 11.33 (s, 1H, NH exchangeable by D$_2$O); ^{13}C NMR (76 MHz DMSO-d_6): δ/ppm 177.66 (C=S), 160.72 (C-OMe), 152.47 (C=O), 144.63 (C=N), 142.40 (C=C), 134.87, 132.95, 130.03, 128.94, 128.13, 127.72, 127.63, 127.44, 126.75, 55.26 (C-OMe); Anal. Calcd. For C$_{18}$H$_{15}$Cl$_2$N$_5$O$_2$S (435.03): C, 49.55; H, 3.47, N; 16.05. Found: C, 49.78; H, 3.84; N, 16.37.

Antimicrobial activity

The in vitro antibacterial activity against two gram-positive strains as *S. aureus* (RCMB010010) and *B. subtilis* (RCMB 015), and two gram-negative strains as *E. coli* (RCMB010052) and *P. vulgaris* (RCMB004) by agar well diffusion method according to the previously reported methods [54, 55, 69].

DFT calculation

All the theoretical calculation were performed using DFT/B3LYP method with a basic set 6-31 g (d) and Gaussian 9.0 package and Gaussian view 6.0.16 software. Additionally, the energy descriptors involving E$_{HOMO}$, E$_{LUMO}$, energy bandgap, ionization potential, electron affinity, electronegativity, chemical hardness, chemical softness, chemical potential, and electrophilic index were calculated as described previously [70].

Molecular docking study

The docking process was performed using Molecular operating Environmental (MOE) 10.2008, Chemical computing Group Inc, Montreal, Quench, Canada [71, 72] according

to the previously reported method. The most active derivatives **3a**, **4a**, **4b**, **9**, and **16** were docked inside the active site of topoisomerase IV (PDB:3FV5). The crystal structure of *E. coli* topoisomerase IV (PDB:3FV5) was retractive and downloaded from the protein data bank (https://www.rcsb.org/structure/3fv5). Subsequently, the protein structure in pdb format was exported to MOE 10.2008 software. The active site was generated according to standard protocol and according to previously reported method [64], where only one chain was sellected. The missed hydrogen was added, the protein was minimized, refined, and redocked using the original ligand that exerted binding energy S = -23.60 kcal/mol with RMSD = 0.828 Å. The most active derivatives **3a**, **4a**, **4b**, **9**, and **16** were drawn and exported to MOE involving added hydrogen, energy minimized using forcefield MMFF94X, and finally saved as a new database. The docking process performed using the trigonal matcher placement and refinement forcefield.

References

1. R. Wang, X. Yin, Y. Zhang, W. Yan, Design, synthesis and antimicrobial evaluation of propylene-tethered ciprofloxacin-isatin hybrids. Eur. J. Med. Chem. **156**, 580–586 (2018). https://doi.org/10.1016/j.ejmech.2018.07.025

2. Y. Hu, S. Zhang, Z. Xu, Z. Lv, M. Liu, 4-Quinolone hybrids and their antibacterial activities. Eur. J. Med. Chem. **141**, 335–345 (2017). https://doi.org/10.1016/j.ejmech.2017.09.050

3. R. Hasan, M. Acharjee, R. Noor, Prevalence of vancomycin resistant Staphylococcus aureus (VRSA) in methicillin resistant *S. aureus* (MRSA) strains isolated from burn wound infections. Tzu Chi Med. J. **28**, 49–53 (2016). https://doi.org/10.1016/j.tcmj.2016.03.002

4. Y.A. Ammar, S.Y. Abbas, M.M. Ghorab, M.S. Al Said, Trans-monocyanoacetylation of phenylenediamines: a simple and efficient synthesis of novel N-(aminophenyl)-2-cyanoacetamides and their derivatives. Tetrahedron Lett. **57**, 275–277 (2016). https://doi.org/10.1016/j.tetlet.2015.11.098

5. A.A. Fadda, S. Bondock, R. Rabie, H.A. Etman, Cyanoacetamide derivatives as synthons in heterocyclic synthesis. Turkish J. Chem. **32**, 259–286 (2008)

6. P.P. Pandey, Pyridine, BoD–Books on Demand, 2018.

7. H. Ashihara, I.A. Ludwig, R. Katahira, T. Yokota, T. Fujimura, A. Crozier, Trigonelline and related nicotinic acid metabolites: occurrence, biosynthesis, taxonomic considerations, and their roles in planta and in human health. Phytochem. Rev. **14**, 765–798 (2015). https://doi.org/10.1007/s11101-014-9375-z

8. Y. Hamada, H.D. Tagad, Y. Nishimura, S. Ishiura, Y. Kiso, Tripeptidic BACE1 inhibitors devised by in-silico conformational structure-based design. Bioorg. Med. Chem. Lett. **22**, 1130–1135 (2012). https://doi.org/10.1016/j.bmcl.2011.11.102

9. A. Malani, A. Makwana, J. Monapara, I. Ahmad, H. Patel, N. Desai, Synthesis, molecular docking, DFT study, and in vitro antimicrobial activity of some 4-(biphenyl-4-yl)-1,4-dihydropyridine and 4-(biphenyl-4-yl)pyridine derivatives. J. Biochem. Mol. Toxicol. (2021). https://doi.org/10.1002/jbt.22903

10. N.C. Desai, H. Somani, A. Trivedi, K. Bhatt, L. Nawale, V.M. Khedkar, P.C. Jha, D. Sarkar, Synthesis, biological evaluation and molecular docking study of some novel indole and pyridine based 1,3,4-oxadiazole derivatives as potential antitubercular agents. Bioorg. Med. Chem. Lett. **26**, 1776–1783 (2016). https://doi.org/10.1016/j.bmcl.2016.02.043

11. F.A. Bassyouni, H.A. Tawfik, A.M. Soliman, M.A. Rehim, Synthesis and anticancer activity of some new pyridine derivatives. Res. Chem. Intermed. **38**, 1291–1310 (2012). https://doi.org/10.1007/s11164-011-0413-9

12. B. Martinez-Gualda, S.-Y. Pu, M. Froeyen, P. Herdewijn, S. Einav, S. De Jonghe, Structure-activity relationship study of the pyridine moiety of isothiazolo[4,3-b]pyridines as antiviral agents targeting cyclin G-associated kinase. Bioorg. Med. Chem. **28**, 115188 (2020). https://doi.org/10.1016/j.bmc.2019.115188

13. A. Ragab, S.A. Fouad, O.A.A. Ali, E.M. Ahmed, A.M. Ali, A.A. Askar, Y.A. Ammar, Sulfaguanidine Hybrid with Some New Pyridine-2-One Derivatives: Design Synthesis, and Antimicrobial Activity against Multidrug-Resistant Bacteria as Dual DNA Gyrase and DHFR Inhibitors. Antibiotics **10**, 162 (2021). https://doi.org/10.3390/antibiotics10020162

14. A. Chaubey, S.N. Pandeya, Pyridine" a versatile nucleuse in pharmaceutical field. Asian J. Pharm. Clin. Res. **4**, 5–8 (2011)

15. A. Kamboj, B. Sihag, D.S. Brar, A. Kaur, D.B. Salunke, Structure activity relationship in β-carboline derived anti-malarial agents. Eur. J. Med. Chem. **221**, 113536 (2021). https://doi.org/10.1016/j.ejmech.2021.113536

16. A. Mehanna, Antidiabetic agents: past, present and future. Future Med. Chem. **5**, 411–430 (2013). https://doi.org/10.4155/fmc.13.13

17. S.M. Gomha, Z.A. Muhammad, M.R. Abdel-aziz, H.M. Abdel-aziz, H.M. Gaber, M.M. Elaasser, One-pot synthesis of new thiadiazolyl-pyridines as anticancer and antioxidant agents. J. Heterocycl. Chem. **55**, 530–536 (2018). https://doi.org/10.1002/jhet.3088

18. J.-F. Renard, F. Lecomte, P. Hubert, X. de Leval, B. Pirotte, N-(3-Arylaminopyridin-4-yl)alkanesulfonamides as pyridine analogs of nimesulide: Cyclooxygenases inhibition, anti-inflammatory studies and insight on metabolism. Eur. J. Med. Chem. **74**, 12–22 (2014). https://doi.org/10.1016/j.ejmech.2013.12.033

19. A.A. Bekhit, A.M. Baraka, Novel milrinone analogs of pyridine-3-carbonitrile derivatives as promising cardiotonic agents. Eur. J. Med. Chem. **40**, 1405–1413 (2005). https://doi.org/10.1016/j.ejmech.2005.06.005

20. N. Bharti, M.R. Maurya, F. Naqvi, A. Azam, Synthesis and antiamoebic activity of new cyclooctadiene ruthenium(II) complexes with 2-acetylpyridine and benzimidazole derivatives.

Bioorg. Med. Chem. Lett. **10**, 2243–2245 (2000). https://doi.org/10.1016/S0960-894X(00)00446-7

21. B. Wu, V. Oesker, J. Wiese, R. Schmaljohann, J.F. Imhoff, Two new antibiotic pyridones produced by a marine fungus, Trichoderma sp. strain MF106. Mar. Drugs. **12**, 1208–1219 (2014). https://doi.org/10.3390/md12031208

22. Y. Yan, X. Li, C. Zhang, L. Lv, B. Gao, M. Li, Research progress on antibacterial activities and mechanisms of natural alkaloids: a review. Antibiot. (2021). https://doi.org/10.3390/antibiotics10030318

23. N.C. Desai, B.Y. Patel, B.P. Dave, Synthesis and antimicrobial activity of novel quinoline derivatives bearing pyrazoline and pyridine analogues. Med. Chem. Res. **26**, 109–119 (2017). https://doi.org/10.1007/s00044-016-1732-6

24. L.J. Piddock, R.N. Walters, J.M. Diver, Correlation of quinolone MIC and inhibition of DNA, RNA, and protein synthesis and induction of the SOS response in Escherichia coli. Antimicrob. Agents Chemother. **34**, 2331–2336 (1990). https://doi.org/10.1128/AAC.34.12.2331

25. A. Titi, M. Messali, B.A. Alqurashy, R. Touzani, T. Shiga, H. Oshio, M. Fettouhi, M. Rajabi, F.A. Almalki, T. Ben Hadda, Synthesis, characterization, X-Ray crystal study and bioctivities of pyrazole derivatives: Identification of antitumor, antifungal and antibacterial pharmacophore sites. J. Mol. Struct. **1205**, 127625 (2020). https://doi.org/10.1016/j.molstruc.2019.127625

26. S.O. Ojwach, J. Darkwa, Pyrazole and (pyrazol-1-yl)metal complexes as carbon–carbon coupling catalysts, Inorganica Chim. Acta. **363**, 1947–1964 (2010). https://doi.org/10.1016/j.ica.2010.02.014

27. A. Jamwal, A. Javed, V. Bhardwaj, A review on pyrazole derivatives of pharmacological potential. J. Pharm. BioSci. **3**, 114–123 (2013)

28. S.T. Heller, S.R. Natarajan, Rapid access to pyrazolo[3,4-c] pyridines via alkyne annulation: limitations of steric control in nickel-catalyzed alkyne insertions. Org. Lett. **9**, 4947–4950 (2007). https://doi.org/10.1021/ol701784w

29. J. Zhang, Y. Zhang, W.F.K. Schnatter, J.W. Herndon, Coupling of N-Heterocycle-Fused Enyne Aldehydes with γ, δ-Unsaturated Fischer Carbene Complexes. Organometallics **25**, 1279–1284 (2006). https://doi.org/10.1021/om051008q

30. S.F. Vasilevsky, E.V. Mshvidobadze, V.I. Mamatyuk, G.V. Romanenko, J. Elguero, Unexpected results in the heterocyclization of 5-acetylenylpyrazole-4-carboxylic acid hydrazides under the influence of CuCl: formation of a diazepinone and dehydrodimerization into the corresponding bis(pyrazolo[4,3-d][1,2]diazepinone). Tetrahedron Lett. **46**, 4457–4459 (2005). https://doi.org/10.1016/j.tetlet.2005.04.127

31. A.R. Katritzky, M. Wang, S. Zhang, M.V. Voronkov, P.J. Steel, Regioselective synthesis of polysubstituted pyrazoles and isoxazoles. J. Org. Chem. **66**, 6787–6791 (2001). https://doi.org/10.1021/jo0101407

32. S.M.M.R. In, Comprehensive Heterocyclic Chemistry II Vol. 3: Katritzky AR. Rees CW. Scriven EFV, (1996).

33. A.S. Hassan, A.A. Askar, A.M. Naglah, A.M. Naglah, A.A. Almehizia, A.A. Almehizia, A. Ragab, Discovery of new schiff bases tethered pyrazole moiety: design, synthesis, biological evaluation, and molecular docking study as dual targeting DHFR/DNA gyrase inhibitors with immunomodulatory activity. Molecules **25**, 2593 (2020). https://doi.org/10.3390/molecules25112593

34. A. Masih, A.K. Agnihotri, J.K. Srivastava, N. Pandey, H.R. Bhat, U.P. Singh, Discovery of novel pyrazole derivatives as a potent anti-inflammatory agent in RAW264.7 cells via inhibition of NF-κB for possible benefit against SARS-CoV-2. J. Biochem. Mol. Toxicol. **35**, e22656 (2021). https://doi.org/10.1002/jbt.22656

35. S.S. Abd El-Karim, H.S. Mohamed, M.F. Abdelhameed, A. El-Galil, E. Amr, A.A. Almehizia, E.S. Nossier, Design, synthesis and molecular docking of new pyrazole-thiazolidinones as potent anti-inflammatory and analgesic agents with TNF-α inhibitory activity. Bioorg. Chem. **111**, 104827 (2021). https://doi.org/10.1016/j.bioorg.2021.104827

36. M. Abdel-Aziz, G.E.-D.A. Abuo-Rahma, A.A. Hassan, Synthesis of novel pyrazole derivatives and evaluation of their antidepressant and anticonvulsant activities. Eur. J. Med. Chem. **44**, 3480–3487 (2009). https://doi.org/10.1016/j.ejmech.2009.01.032

37. M.M.S. Wassel, W.M.G. El-din, A. Ragab, G.A.M.E. Ali, Y.A. Ammar, Antiviral activity of adamantane-pyrazole derivatives against foot and mouth disease virus infection in vivo and in vitro with molecular docking study. J. Appl. Vet. Sci. **5**, 37–46 (2020). https://doi.org/10.21608/JAVS.2020.118001

38. M.M.S. Wassel, A. Ragab, G.A.M. Elhag Ali, A.B.M. Mehany, Y.A. Ammar, Novel adamantane-pyrazole and hydrazone hybridized: design, synthesis, cytotoxic evaluation, SAR study and molecular docking simulation as carbonic anhydrase inhibitors. J. Mol. Struct. **1223**, 128966 (2020). https://doi.org/10.1016/j.molstruc.2020.128966

39. K.Y. Lee, J.M. Kim, J.N. Kim, Regioselective synthesis of 1,3,4,5-tetrasubstituted pyrazoles from Baylis-Hillman adducts. Tetrahedron Lett. **44**, 6737–6740 (2003). https://doi.org/10.1016/S0040-4039(03)01648-4

40. H. Ali Mohamed, Y.A. Ammar, G.A.M. Elhagali, H.A. Eyada, D.S. Aboul-Magd, A. Ragab, In vitro antimicrobial evaluation, single-point resistance study, and radiosterilization of novel pyrazole incorporating thiazol-4-one/thiophene derivatives as dual DNA gyrase and DHFR inhibitors against MDR pathogens. ACS Omega (2022). https://doi.org/10.1021/acsomega.1c05801

41. H.F. Rizk, M.A. El-Borai, A. Ragab, S.A. Ibrahim, M.E. Sadek, A novel of azo-thiazole moiety alternative for benzidine-based pigments: design, synthesis, characterization, biological evaluation, and molecular docking study. Polycycl. Aromat. Compd. (2021). https://doi.org/10.1080/10406638.2021.2015402

42. A. Ezzat, M.B.I. Mohamed, A.M. Mahmoud, R.S. Farag, A.S. El-Tabl, A. Ragab, Synthesis, spectral characterization, antimicrobial evaluation and molecular docking studies of new Cu (II), Zn (II) thiosemicarbazone based on sulfonyl isatin. J. Mol. Struct. **1251**, 132004 (2022). https://doi.org/10.1016/j.molstruc.2021.132004

43. E.S.A.E.H. Khattab, A. Ragab, M.A. Abol-Ftouh, A.A. Elhenawy, Therapeutic strategies for Covid-19 based on molecular docking and dynamic studies to the ACE-2 receptors, Furin, and viral spike proteins. J. Biomol. Struct. Dyn. **40**, 1–19 (2022). https://doi.org/10.1080/07391102.2021.1989036

44. S.A. Ibrahim, A. Ragab, H.A. El-Ghamry, Coordination compounds of pyrazolone-based ligand: design, characterization, biological evaluation, antitumor efficiency, and DNA binding evaluation supported by in silico studies. Appl. Organomet. Chem. **36**, 1–17 (2022). https://doi.org/10.1002/aoc.6508

45. Y.A. Ammar, M.M. Aly, A.A.G. Al-Sehemi, M.A. Salem, M.S.A. El-Gaby, Cyanoacetanilides intermediates in heterocyclic synthesis. Part 5: preparation of hitherto unknown 5-aminopyrazole and pyrazolo [1, 5-a] pyrimidine derivatives containing sulfamoyl moiety. J. Chin. Chem. Soc. **56**, 1064–1071 (2009)

46. Y.A. Ammar, M.S.A. El-Gaby, M.A. Salem, Cyanoacetanilides intermediates in heterocyclic synthesis. Part 6: Preparation of some hitherto unknown 2-oxopyridine, bipyridine, isoquinoline and chromeno[3,4-c]pyridine containing sulfonamide moiety. Arab. J. Chem. **7**, 615–622 (2014). https://doi.org/10.1016/j.arabjc.2013.11.026

47. P. Wang, S.M. Batt, B. Wang, L. Fu, R. Qin, Y. Lu, G. Li, G.S. Besra, H. Huang, Discovery of novel thiophene-arylamide derivatives as DprE1 inhibitors with potent antimycobacterial activities. J. Med. Chem. **64**, 6241–6261 (2021). https://doi.org/10.1021/acs.jmedchem.1c00263

48. S.T. Cheung, M.S. Miller, R. Pacoma, J. Roland, J. Liu, A.M. Schumacher, L.C. Hsieh-Wilson, Discovery of a small-molecule modulator of glycosaminoglycan sulfation. ACS Chem. Biol. **12**, 3126–3133 (2017). https://doi.org/10.1021/acschembio.7b00885

49. M. Hajjami, F. Ghorbani, S. Rahimipanah, S. Roshani, Efficient preparation of Zr(IV)-salen grafted mesoporous MCM-41 catalyst for chemoselective oxidation of sulfides to sulfoxides and Knoevenagel condensation reactions. Chin. J. Catal. **36**, 1852–1860 (2015). https://doi.org/10.1016/S1872-2067(15)60968-8

50. A.S. Hassan, N.M. Morsy, H.M. Awad, A. Ragab, Synthesis, molecular docking, and in silico ADME prediction of some fused pyrazolo[1,5-a]pyrimidine and pyrazole derivatives as potential antimicrobial agents. J. Iran. Chem. Soc. **19**, 521–545 (2022). https://doi.org/10.1007/s13738-021-02319-4

51. H.F. Rizk, M.A. El-Borai, A. Ragab, S.A. Ibrahim, Design, synthesis, biological evaluation and molecular docking study based on novel fused pyrazolothiazole scaffold. J. Iran. Chem. Soc. **17**, 2493–2505 (2020). https://doi.org/10.1007/s13738-020-01944-9

52. D. Secci, A. Bolasco, P. Chimenti, S. Carradori, The state of the art of pyrazole derivatives as monoamine oxidase inhibitors and antidepressant/anticonvulsant agents. Curr. Med. Chem. **18**, 5114–5144 (2011)

53. S. Singh Jadav, B. Nayan Sinha, B. Pastorino, X. de Lamballerie, R. Hilgenfeld, V. Jayaprakash, Identification of pyrazole derivative as an antiviral agent against Chikungunya through HTVS. Lett. Drug Des. Discov. **12**, 292–301 (2015)

54. Y.A. Ammar, S.M.A.A. El-Hafez, S.A. Hessein, A.M. Ali, A.A. Askar, A. Ragab, One-pot strategy for thiazole tethered 7-ethoxy quinoline hybrids: synthesis and potential antimicrobial agents as dihydrofolate reductase (DHFR) inhibitors with molecular docking study. J. Mol. Struct. **1242**, 130748 (2021). https://doi.org/10.1016/j.molstruc.2021.130748

55. D.M. Elsisi, A. Ragab, A.A. Elhenawy, A.A. Farag, A.M. Ali, Y.A. Ammar, Experimental and theoretical investigation for 6-Morpholinosulfonylquinoxalin-2(1H)-one and its haydrazone derivate: synthesis, characterization, tautomerization and antimicrobial evaluation. J. Mol. Struct. **1247**, 131314 (2022). https://doi.org/10.1016/j.molstruc.2021.131314

56. A. Ragab, D.M. Elsisi, O.A. Abu Ali, M.S. Abusaif, A.A. Askar, A.A. Farag, Y.A. Ammar, Design, synthesis of new novel quinoxalin-2(1H)-one derivatives incorporating hydrazone, hydrazine, and pyrazole moieties as antimicrobial potential with in-silico ADME and molecular docking simulation. Arab. J. Chem. **15**, 103497 (2022). https://doi.org/10.1016/j.arabjc.2021.103497

57. M. Erol, I. Celik, E. Uzunhisarcikli, G. Kuyucuklu, Synthesis, molecular docking, and DFT studies of some new 2,5-disubstituted benzoxazoles as potential antimicrobial and cytotoxic agents. Polycycl. Aromat. Compd. (2020). https://doi.org/10.1080/10406638.2020.1802305

58. A.Y. Alzahrani, Y.A. Ammar, M. Abu-Elghait, M.A. Salem, M.A. Assiri, T.E. Ali, A. Ragab, Development of novel indolin-2-one derivative incorporating thiazole moiety as DHFR and quorum sensing inhibitors: synthesis, antimicrobial, and antibiofilm activities with molecular modelling study. Bioorg. Chem. **119**, 105571 (2022). https://doi.org/10.1016/j.bioorg.2021.105571

59. S.A. Khan, A.M. Asiri, H.M. Basisi, M. Asad, M.E.M. Zayed, K. Sharma, M.Y. Wani, Synthesis and evaluation of quinoline-3-carbonitrile derivatives as potential antibacterial agents. Bioorg. Chem. **88**, 102968 (2019). https://doi.org/10.1016/j.bioorg.2019.102968

60. I. Celik, M. Erol, O. Temiz Arpaci, F. Sezer Senol, I. Erdogan Orhan, Evaluation of activity of some 2,5-disubstituted benzoxazole derivatives against acetylcholinesterase, butyrylcholinesterase and tyrosinase: ADME prediction, DFT and comparative molecular docking studies. Polycycl. Aromat. Compd. **42**, 412–423 (2022). https://doi.org/10.1080/10406638.2020.1737827

61. M.M.S. Wassel, Y.A. Ammar, G.A.M. Elhag Ali, A. Belal, A.B.M. Mehany, A. Ragab, Development of adamantane scaffold containing 1,3,4-thiadiazole derivatives: design, synthesis, anti-proliferative activity and molecular docking study targeting EGFR. Bioorg. Chem. **110**, 104794 (2021). https://doi.org/10.1016/j.bioorg.2021.104794

62. S.A. Ibrahim, H.F. Rizk, D.S. Aboul-Magd, A. Ragab, Design, synthesis of new magenta dyestuffs based on thiazole azomethine disperse reactive dyes with antibacterial potential on both dyes and gamma-irradiated dyed fabric. Dye. Pigment. **193**, 109504 (2021). https://doi.org/10.1016/j.dyepig.2021.109504

63. E.A. Fayed, Y.A. Ammar, M.A. Saleh, A.H. Bayoumi, A.B.M. Mehany, A. Ragab, Design, synthesis, antiproliferative evaluation, and molecular docking study of new quinoxaline derivatives as apoptotic inducers and EGFR inhibitors. J. Mol. Struct. **1236**, 130317 (2021). https://doi.org/10.1016/j.molstruc.2021.130317

64. M.O. Puskullu, I. Celik, M. Erol, H. Fatullayev, E. Uzunhisarcikli, G. Kuyucuklu, Antimicrobial and antiproliferative activity studies of some new quinoline-3-carbaldehyde hydrazone derivatives. Bioorg. Chem. **101**, 104014 (2020). https://doi.org/10.1016/j.bioorg.2020.104014

65. M.A. Salem, A. Ragab, A.A. Askar, A. El-Khalafawy, A.H. Makhlouf, One-pot synthesis and molecular docking of some new spiropyranindol-2-one derivatives as immunomodulatory agents and in vitro antimicrobial potential with DNA gyrase inhibitor. Eur. J. Med. Chem. **188**, 111977 (2020). https://doi.org/10.1016/j.ejmech.2019.111977

66. A.R.Y.A. Ammar, A.MSh. El-Sharief, A. Belal, S.Y. Abbas, Y.A. Mohamed, A.B.M. Mehany, Design, synthesis, antiproliferative activity, molecular docking and cell cycle analysis of some novel (morpholinosulfonyl) isatins with potential EGFR inhibitory activity. Eur. J. Med. Chem. **156**, 918–932 (2018). https://doi.org/10.1016/j.ejmech.2018.06.061

67. E.A. Fayed, A. Ragab, R.R. Ezz Eldin, A.H. Bayoumi, Y.A. Ammar, In vivo screening and toxicity studies of indolinone incorporated thiosemicarbazone, thiazole and piperidinosulfonyl moieties as anticonvulsant agents. Bioorg. Chem. (2021). https://doi.org/10.1016/j.bioorg.2021.105300

68. S.A. Ibrahim, E.A. Fayed, H.F. Rizk, S.E. Desouky, A. Ragab, Hydrazonoyl bromide precursors as DHFR inhibitors for the synthesis of bis-thiazolyl pyrazole derivatives; antimicrobial activities, antibiofilm, and drug combination studies against MRSA. Bioorg. Chem. **116**, 105339 (2021). https://doi.org/10.1016/j.bioorg.2021.105339

69. A. Ragab, Y.A. Ammar, A. Ezzat, A.M.M.M.B.I. Mohamed, A.S. El-Tabl, R.S. Farag, Synthesis, characterization, thermal properties, antimicrobial evaluation, ADMET study, and molecular docking simulation of new mono Cu (II) and Zn (II) complexes with 2-oxoindole derivatives. Comput. Biol. Med. **145**, 105473 (2022). https://doi.org/10.1016/j.compbiomed.2022.105473

70. A.Y. Alzahrani, Y.A. Ammar, M.A. Salem, M. Abu-Elghait, A. Ragab, Design, synthesis, molecular modeling, and antimicrobial potential of novel 3-[(1H-pyrazol-3-yl)imino]indolin-2-one derivatives as DNA gyrase inhibitors. Arch. Pharm. (Weinheim) **355**, e2100266 (2022). https://doi.org/10.1002/ardp.202100266

71. M. Eldeeb, E.F. Sanad, A. Ragab, Y.A. Ammar, K. Mahmoud, M.M. Ali, N.M. Hamdy, Anticancer effects with molecular docking confirmation of newly synthesized Isatin sulfonamide molecular hybrid derivatives against hepatic cancer cell lines. Biomedicines (2022). https://doi.org/10.3390/biomedicines10030722

72. E.A. El-Kalyoubi, S.A.; Ragab, A.; Abu Ali, O.A.; Ammar, Y.A.; Seadawy, M.G.; Ahmed, A.; Fayed, One-Pot Synthesis and Molecular Modeling Studies of New Bioactive Spiro-Oxindoles Based on Uracil Derivatives as SARS-CoV-2 Inhibitors Targeting RNA Polymerase and Spike Glycoprotein, Pharm. Artic. 15 (2022). https://doi.org/10.3390/ph15030376 Academic.